

Highlights of Joint Research

Synchrotron Radiation Laboratory

The Synchrotron Radiation Laboratory (SRL) was established in 1975 as a research group dedicating to solid state physics using synchrotron radiation. In 1989, the SRL started to hold the Tsukuba branch, a branch laboratory in the Photon Factory (PF), High Energy Accelerator Research Organization (KEK). The SRL consists of the accelerator physics group and the solid state spectroscopy group. The members of the accelerator group have been carrying out research works on the accelerator physics and developing various new accelerator related technology in collaboration with other SR facilities. The accelerator group studied future ERL (energy recovery linac) light sources and developed ERL components in collaboration with KEK, AIST and JAEA, main works of which are carried out both in Kashiwa campus and at KEK in Tsukuba.

The spectroscopy group has been not only serving users at the Tsukuba branch with technical supports and advices, but also carrying out their own research works on advanced solid state spectroscopy. SRL maintains a Revolver undulator, two beamlines and three experimental stations; BL-18A for angle-resolved photoemission spectroscopy with SCIENTA SES100 energy analyser and undulator beamlines, BL-19A and BL-19B, for spin- and angle-resolved photoelectron spectroscopy (SARPES) and soft X-ray emission spectroscopy experiments, respectively. They are fully opened to outside users for experiments using high brilliant synchrotron radiation. The operation time of these beamlines are about 4000 hours and the number of users is more than 100 a year. In 2009, the new spin detector utilizing VLEED has been utilized to investigate those, such as topological insula-

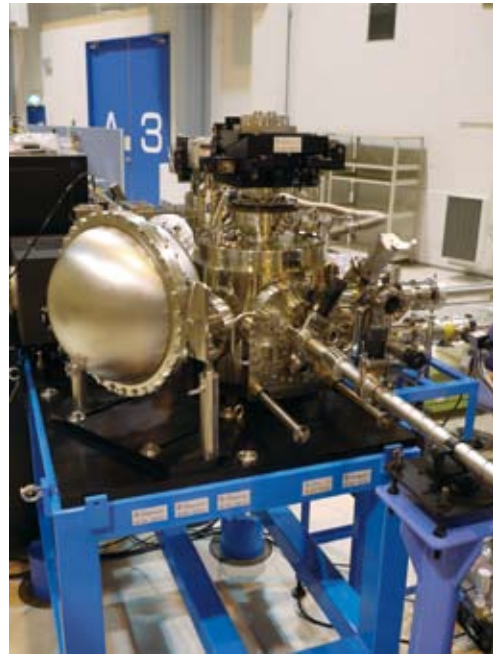


Fig.2. ARPES spectrometer for 3D analyses of electronic structures of nano-fabricated materials

tors and quantum films with Rashba splitting surface states, which have been the exciting topics in surface and solid state physics and strongly demand high resolution spin-resolved photoemission spectra. The new system at BL-19A has accepted many users including those with urgent proposals from Korea and China.

The staff members of SRL also participate to the Materials Research Division of the Synchrotron Radiation Research Organization of the University of Tokyo (SRRO) and play essential roles in promoting scientific activities at a new soft X-ray undulator beamline at the SPring-8, BL07-LSU. The beamline consists of four horizontal



Fig. 1. Time-resolved soft X-ray spectrometer installed at BL07LSU



Fig.3. High resolution soft X-ray emission spectrometer at BL07LSU

figure-8 undulators and varied line spacing plain grating monochromator which covers the energy range between 250 eV and 2 keV, and is equipped with experimental apparatuses using high brilliance synchrotron radiation in soft X-ray region. Three experimental apparatuses are installed at the beamline. They are for time-resolved soft X-ray spectroscopy, three-dimensional analyses of electronic structures of nano-fabricated materials and soft X-ray emission spectroscopy of bio-materials, which are become available for outside users in October, 2009. The four vertical figure-8 undulator segments were already constructed and will be inserted into the 25-m long straight section of SPring-8 in summer of 2010, and the polarization controlled undulator light will be available from the beginning of 2011.

Supercomputer Center

The Supercomputer Center (SCC) is a part of the Materials Design and Characterization Laboratory (MDCL) of ISSP. Its mission is to serve the whole community of computational condensed-matter physics of Japan by providing it with high performance computing environment. In particular, the SCC selectively promotes and supports large-scale computations. For this purpose, the SCC invites proposals for supercomputer-aided research projects and hosts the Steering Committee, as mentioned below, that evaluates the proposals.

Until March 2009, the SCC has been operating two super-computers, systems A and B. System A is Hitachi SR11000/48 that consists of 48 high performance nodes composed of tightly-coupled microprocessors. With the aid of the automatic parallelization of FORTRAN compiler, a node of System A can be used as if it were a single-processor computer. System A has 2.8 TB memory and achieves 5.8 TFlops peak performance in total. On the other hand, System B, which is SGI Altix 3700/1280, is a parallel supercomputer with relatively loose coupling. It consists of 19 nodes inter-connected by a gigabit Ethernet network. Each node is a computer with 64 GB distributed-shared-memory and consists of 64 Intel Itanium 2 CPUs inter-connected by a high performance network. System B achieves 7.7 TFlops total throughput performance.

The school year 2010 will be a year of big steps forward for the SCC. The SCC is replacing the two supercomputer systems. The new system B will be SGI Altix ICE 8400EX, which consists of 30 racks or 15360 cores whereas the new system A will be NEC SX-9, which consists of 4 nodes or 64 cpus. These machines will be available in July, 2010, which will provide the computational condensed-matter physics community with more than 15 times greater computational resources than the old systems. Moreover, the ISSP will be hosting Computational Materials Science Initiative (CMSI), a new activity of promoting materials science study with next-generation parallel supercomputing. In CMSI, a number of major Japanese research institutes in various branches of materials science will be involved.

All staff members of university faculties or public research institutes in Japan are invited to propose research projects (called User Program). The proposals are evaluated by the Steering Committee of SCC. Pre-reviewing is done by the Supercomputer Project Advisory Committee. In school

year 2009 totally 181 projects were approved. The total points applied and approved are listed in Table. 1 below.

The research projects are roughly classified into the following three categories (the number of projects approved is indicated in the parenthesis):

- First-Principles Calculation of Materials Properties (64)
- Strongly Correlated Quantum Systems (60)
- Cooperative Phenomena in Complex, Macroscopic Systems (57)

All the three involve both methodology of computation and its applications. The results of the projects are reported in the booklet 'Activity Report 2009' of the SCC. Every year 3-4 projects are selected for "invited papers" and published as the first papers in the Activity Report. In the Activity Report 2009, the following three invited papers are included:

- "Large-Scale Density Functional Calculations that Reveal Physics and Chemistry in Nano Structures",
Atsushi OSHIYAMA and Jun-ichi IWARA
- "Monte Carlo Study of a Mesoscopic Capacitor",
Takeo KATO
- "Coarse-Grained Molecular Dynamics Simulation Approach for Polymer Nano-Composites Rubber",
Katsumi HAGITA

Class	Max/Min Points	Application	Number of Projects	Total Points			
				Applied		Approved	
				System A	System B	System A	System B
A	<100K	any time	2	200K	0K	200K	0K
B	<2M	twice a year	46	46M	43M	39M	36M
C	<20M	twice a year	128	1256M	956M	1087M	844M
D		any time	5	68M	62M	65M	59M
S	>20M	twice a year	0	0M	0M	0M	0M
Total			181	1370M	1061M	1191M	939M

Table 1. Research projects approved in 2009. The maximum points allotted to the project of each class are the sum of the points for the two systems; 1 K point of System-A corresponds to charge for 0.37 hours \times node, while the corresponding figure is 0.22 hours \times 64CPU for System-B.

Neutron Science Laboratory

The Neutron Scattering Laboratory (NSL) has been playing a central role in neutron scattering activities in Japan since 1961 by performing its own research programs as well as providing a strong General User Program for the university-owned various neutron scattering spectrometers installed at the JRR-3 (20MW) operated by Japan Atomic Energy Agency (JAEA) in Tokai. In 2003, the Neutron Scattering Laboratory was reorganized as the Neutron Science Laboratory (NSL) to further promote the neutron science with use of the instruments in JRR-3. Under the General User Program supported by NSL, 14 university-group-owned spectrometers in the JRR-3 reactor are available for a wide scope of researches on material science, and proposals close to 300 are submitted each year, and the number of visiting users under this program reaches over 6000 person-day/



Fig. 1. The reactor hall of JRR-3. The eight neutron scattering instruments are attached to the horizontal beam tubes in the reactor experimental hall. Two thermal and three cold guides are extracted from the reactor core towards the guide hall located to the left.

year. In 2009, NSL and Neutron Science Laboratory (KENS), High Energy Accelerator Research Organization (KEK) built a chopper spectrometer, High Resolution Chopper Spectrometer, HRC, at the beam line BL12 of MLF/J-PARC (Materials and Life Science Experimental Facility, J-PARC). HRC covers a wide energy and Q-range ($10 \mu\text{eV} < \hbar\omega < 2 \text{ eV}$ and $0.02 \text{ \AA}^{-1} < Q < 50 \text{ \AA}^{-1}$), and therefore becomes complementary to the existing inelastic spectrometers at JRR-3. HRC will start commissioning and trial user experiments through the S-type/IRT-project proposal in FY2010, and is expected to accept general users through the J-PARC proposal system in FY2011.

Triple axis spectrometers, HRC, and a high resolution powder diffractometer are utilized for a conventional solid state physics and a variety of research fields on hard-condensed matter, while in the field of soft-condensed matter science, researches are mostly carried out by using the small angle neutron scattering (SANS-U) and/or neutron spin echo (iNSE) instruments. The upgraded time-of-flight (TOF) inelastic scattering spectrometer is also available through the ISSP-NSL user program.

Major research topics on the hard-condensed matter science cover stripe order in high- T_c superconductors, and closely related 2 dimensional systems, charge and orbital

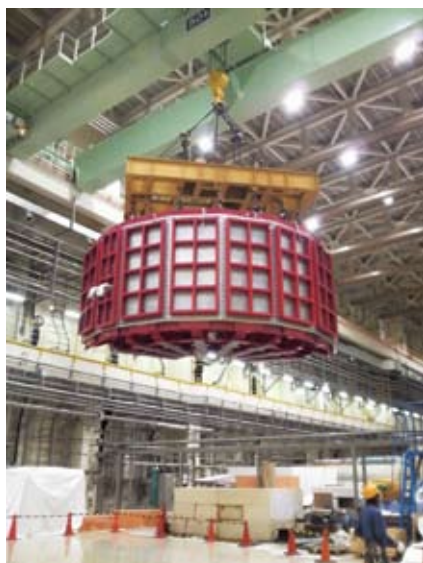


Fig. 2. Installation of vacuum chamber of HRC at MLF/J-PARC.

ordering in CMR manganites, quadrupolar ordering in rare-earth based intermetallic compounds, spin dynamics of low dimensional dimmer systems, etc. On the other hand, the research topics on the soft-condensed matter science cover structural characterization of polymer gels, polymer blends, micelles, amphiphilic polymers, block copolymers, proteins, dynamics of brush-polymers on surface, slow dynamics of surfactants, pressure dependence of dynamics of amphiphilic membranes, and so on. In addition, there are a variety of activities on fundamental physics, neutron beam optics, developments of neutron scattering techniques.

The NSL also operates the U.S.-Japan Cooperative Program on neutron scattering, providing further research opportunities to material scientists who utilize the neutron scattering technique for their research interests.

The activity report on Neutron Scattering Research in JFY2009 is given in NSL-ISSP Activity Report vol. 16 (2009), which can be downloaded from the following URL, http://quasi.issp.u-tokyo.ac.jp/actrep/actrep-16/index-rep_vol16.html.

The list of publication is also given at, http://quasi.issp.u-tokyo.ac.jp/actrep/actrep-16/index-rep_vol16.html.

International MegaGauss Science Laboratory

The aim of this laboratory is to study the physical properties of solid-state materials (such as semiconductors, magnetic materials, metals, insulators, superconducting materials) under ultra-high magnetic field conditions. Such a high magnetic field is also used for controlling the new material phase and functions. Our pulse magnets, at moment, can generate up to 85 Tesla (T) by non-destructive manner, and from 100 up to 730 T (the world strongest as an in-door record) by destructive (the single turn coil and the electromagnetic flux compression) methods.

They are opened for scientists both from Japan and from overseas, especially from Asian countries, and many fruitful results are expected to come out not only from collaborative research but also from our in-house activities. One of our ultimate goals is to provide the scientific users as our joint research with magnets capable of a 100 T, milli-second pulses in a non-destructive mode, and to offer versatile physical precision measurements. The available measuring techniques now involve magneto-optical measurements, cyclotron resonance, spin resonance, magnetization and transport measurements.

Our interests cover the study on quantum phase transitions (QPT) induced by high magnetic fields. Field-induced QPT has been explored in various materials such as quantum spin systems, strongly correlated electron systems and other magnetic materials. Non-destructive strong pulse magnets are expected to provide us with reliable and precise solid state physics measurements. The number of collaborative groups for the research is over 50 in the year of 2009.

A 210 MJ flywheel generator which is the world largest DC power supply has been installed in the newly built DC Flywheel generator station at our Institute. The generator, once disassembled from the one used for Toroidal magnetic field coil in JFT-2M (JAERI Fusion Torus-2M) Tokamak nuclear fusion testing device, is now renewed as a power

supply for the pulse magnets. The construction of the magnet service station has also been accomplished. The magnet technologies are intensively devoted to the quasi-steady long pulse magnet (an order of 1-10 sec) energized by the giant DC power supply, and also used for the outer-magnet coil to realize a 100 T nondestructive magnet.

Developments of our destructive magnets are currently in progress. The ultra-high magnetic fields are obtained in a microsecond time scale. The electromagnetic flux compression (EMFC) system is equipped with a 5 MJ condenser bank and its seed coils with a 1.5 MJ condenser bank. The protector chamber and iron block protectors were refined against stronger explosion than before endurable for explosion by a full injection of 5 MJ. By devising copper lined primary coil, we could improve energy transfer efficiency from the primary coil to the liner kinetic energy compressing the magnetic flux. The seed field coils providing the initial magnetic flux are also newly designed and the maximum magnetic field was increased from 3.2 T to over 4.4 T at the position of the primary coil. These efforts led us to obtain the maximum magnetic field of 730 T by a 4 MJ injection of the EMFC recognized as a renewal of the world record as an indoor experiment. We have also developed the techniques for application of this extremely high magnetic field to the materials science. The single-turn coil (STC) system provides high fields of up to 200 T rather easily compared to the EMFC by using the energy of 200 kJ. We have two STC systems, one is a horizontal type (H-type) and another is a vertical type (V-type). Various kinds of laser spectroscopy experiments such as the cyclotron resonance and the Faraday rotation using the H-type STC are available. One the other hand, for very low temperature experiment, a combination of the V-type STC and a liquid helium bath cryostat is very useful; the magnetization measurement at 2.5 K can be performed up to 100 T.



Fig. 1. The building for the flywheel generator (right hand side) and a long pulse magnet station (left hand side). The flywheel giant DC generator is 350 ton in weight and 5 m high (bottom). The generator, capable of a 51 mega watt out put power with a 210 mega joule energy storage, is planned to energize the long pulse magnet generating 100 Tesla without destruction.

Spin Transition in a Four-Coordinate Iron Oxide

H. Kageyama, T. Okada, and T. Yagi.

Many iron oxides (*e.g.* iron perovskites, (Mg,Fe)O) exhibit structural/electronic transitions against pressure. Mössbauer spectroscopy revealed a spin transition from $S = 2$ to $S = 1$ in SrFeO₂ containing oxygen square-planes around iron. It is known in general that spin transition involves a reduction of unoccupied 3d orbital so that one can expect a reduction of lattice parameters at the critical pressure. To investigate this change and also possible structural transition, we performed high pressure x-ray diffraction.

Powder X-ray diffraction profiles at high pressures up to 43 GPa were recorded using Mo-K α radiation from a 5.4 kW Rigaku rotating anode generator equipped with a 100 μ m collimator. A powder sample of SrFeO₂ was loaded into a 300 μ m hole of a pre-indented stainless-steel gasket of the diamond-anvil cell. A 4:1 methanol: ethanol mixture was used as the pressure-transmitting medium. The shift of ruby fluorescence was used to determine the pressure. To estimate the pressure distribution along the sample, several ruby chips were placed inside the hole at different distances from its centre. It was found that the pressure gradient at the sample was not more than 0.5 GPa at maximal pressures. The diffracted X-rays were collected with an image plate. Four diffraction peaks, 110, 011, 020 and 121, were used to calculate the cell parameters.

All the peaks of the diffraction patterns at each pressure could be assigned to a tetragonal infinite-layer structure, and no additional reflections were detected within the resolution of the experiment (Figure 1). Although the measured range of the diffraction angles is not sufficient to confirm this fully, it is likely that the transition is isostructural. At pressures below the spin transition, the pressure dependence of the volume can be fitted by the third-order Birch–Murnaghan equation of state with the bulk modulus $K_0 = 126$ GPa. As displayed in Figure 2, the unit cell parameters a and c decrease smoothly with the application of

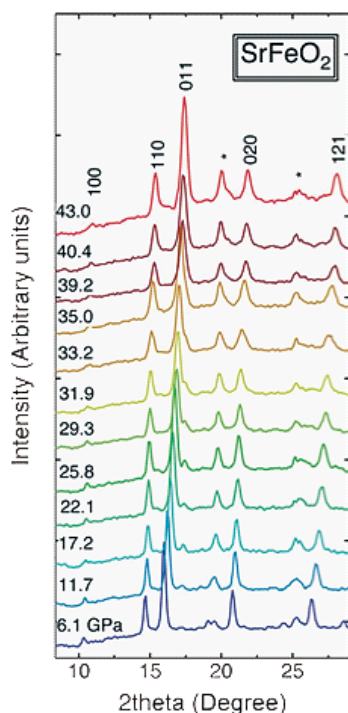


Fig. 1. X-ray diffraction pattern of SrFeO₂ under high pressures.

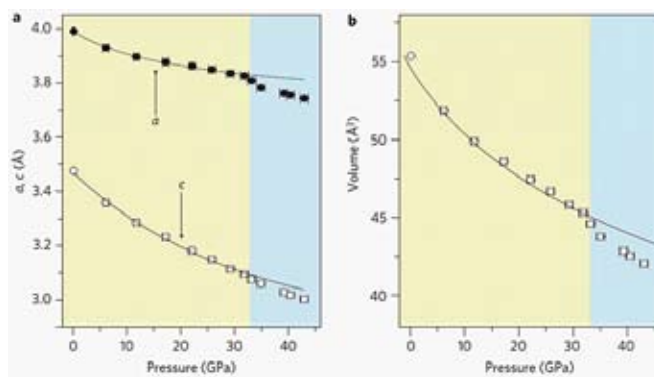


Fig. 2. Evolution of the lattice parameters of SrFeO₂ against pressure (a), Evolution of the volume of SrFeO₂ against pressure (b)

pressure, but exhibit a significant drop at 33 ± 1 GPa, which agrees well with the pressure estimated from the Mössbauer study. Therefore, this anomaly might be associated with the claimed spin transition. A volume reduction of $\sim 3\%$ is comparable with those for other compounds that exhibit high-spin to low-spin transitions.

Using powder x-ray diffraction, we showed that SrFeO₂ under high pressures does not exhibit strong structural change during the spin transition. Moreover we were able to observe the spin transition through a decrease of the volume of the unit cell.

Reference

[1] T. Kawakami *et al.*, Nature Chemistry 1, 371 (2009).

Authors

C. Tassel^a, Y. Tsujimoto^a, H. Kageyama^a, T. Okada, and T. Yagi.

^aKyoto University

Direct Evidence of Surface State Contribution to the Kondo Resonance

Y. Hasegawa, S.-J. Kahng, and Q. K. Xue

The Kondo effect is a many-body phenomenon which results from a correlation of an electron spin in a magnetic impurity with conduction electrons of a host metal. Below the Kondo temperature, a singlet ground state is formed, giving rise to a resonance, called the Kondo resonance, near the Fermi energy at the site of the impurity. Low-temperature scanning tunneling microscopy/spectroscopy (STM/S), which has atomic-scale spatial resolution and meV energy resolution, is an ideal tool to observe the Fano-shaped resonance on a magnetic impurity adsorbed on metal surfaces. So far, most of the Kondo resonance observations by STM/S were performed on noble metal (111) substrates, which have both metallic surface states and the bulk states, and therefore, there have been arguments on the contribution of the surface state to the observed Kondo resonance. In order to provide direct evidence of the surface state contribution to the Kondo resonance, we performed its observation on a surface which has metallic free-electron-like surface states formed on a semiconducting substrate.

An STM image in Figure 1 shows a 5, 10, 15, 20-tetrakis-(4-bromophenyl)-porphyrin-Co (TBrPP-Co) molecule adsorbed on a Si(111)- $\sqrt{3} \times \sqrt{3}$ Ag surface together with Ag adsorbates. Four lobes of the molecule are clearly resolved in the highly resolved image. The Ag-induced reconstructed

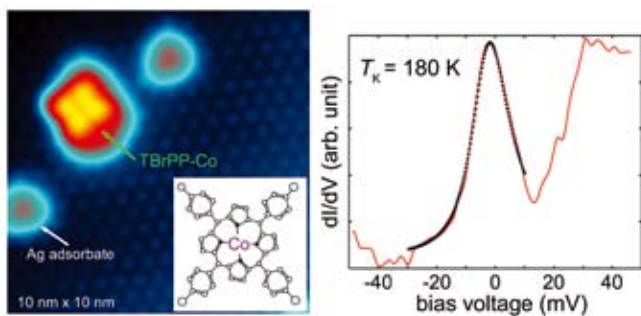


Fig. 1. STM image of a TBrPP-Co molecule adsorbed on a Si(111)- $\sqrt{3} \times \sqrt{3}$ Ag surface and a dI/dV spectrum taken above the molecular center showing a resonance around the Fermi energy.

surface is known to have metallic surface states as revealed by angle-resolved photoemission spectroscopy and standing wave observation with STM/S. Existence of a spin at the central Co atom of the molecule has been confirmed by STM observation of the Kondo resonance on Cu(111) surface.

For the Kondo resonance measurements, we picked up an isolated molecule whose closest Ag adsorbate is more than 5 nm away to minimize the influence of the Ag adsorbates. The right panel in Figure 1 shows a dI/dV spectrum taken above the molecular center, showing a clear peak near the zero bias voltage. The peak can be fitted well with the expected Fano resonance as demonstrated with a dotted fitting line, and from the fitting the Kondo temperature and the Fano interference parameter were given as ~ 180 K and ~ 8 , respectively.

Figure 2 shows a series of dI/dV spectra taken with various lateral tip distances (r) from the molecular center. The resonance peak amplitude decreases with the lateral tip displacement, and up to 1.4 nm the peak is visible. At the distances larger than 2.5 nm, however, the obtained spectra do not have a significant feature near the Fermi energy, like the case on the clean $\sqrt{3} \times \sqrt{3}$ Ag region. We found that the Kondo temperature and the Fano interference parameter are nearly constant in this distance range. Theoretical studies suggested that the Kondo resonance due to bulk states decays rapidly in the lateral direction whereas the surface state contribution stays longer (> 1 nm) from the magnetic impurity. The spectra we observed obviously demonstrate the characteristic slow-decaying features of the surface-state contributing Kondo resonance. The distinct Fano-shaped peak near the Fermi energy and its long decay length observed around the TBrPP-Co molecule adsorbed on

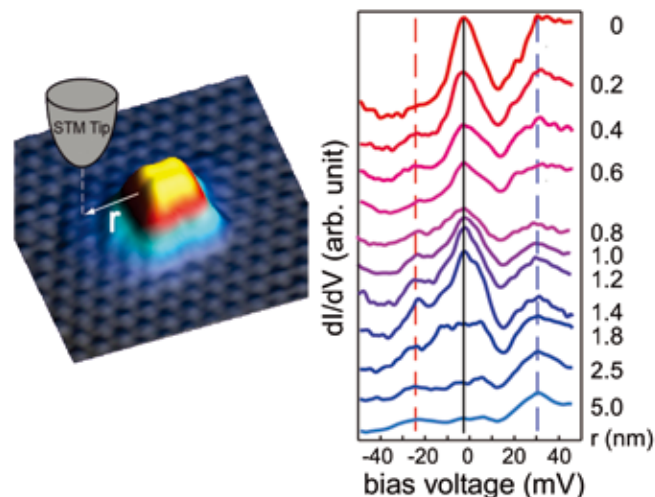


Fig. 2. a series of dI/dV spectra taken with various lateral tip distances (r) from the molecular center.

the bulk-state-absent (near the Fermi energy) substrate are an direct evidence that the surface state does play a significant role in the Kondo resonance.

Reference

[1] Q. Li *et al.*, Jpn. J. Appl. Phys. **48**, 08JB01 (2009); Phys. Rev. B **80**, 115431 (2009).

Authors

Q. Li, S. Yamazaki, T. Eguchi, H. Kim^a, S.-J. Kahng^a, J. F. Jia^b, Q. K. Xue^b, and Y. Hasegawa^a
^a Korea University, Korea
^b Tsinghua University, China

Field-Switchable Metal-Oxide Junctions

I. Ohkubo and M. Lippmaa

The observation of repeatable electric-field-driven switching of the resistance of metal-oxide junctions has prompted the development of resistance random access memory devices, which may allow higher-density non-volatile memories to be constructed for computing and data storage applications. The resistive switching phenomenon is known to appear at a number of oxide interfaces and various mechanisms have been proposed to explain the resistance change, including the formation of conducting filaments and the modification of the electronic or physical structure of an interface. From a solid-state physics point of view, resistive switching systems can be quite difficult to analyze, since the interface layers, while solid, are not static. High applied fields and, in filamentary conduction cases, high local current densities can result in dynamic reduction and oxidation of nanometer-scale regions, where the reaction kinetics are determined by the types of cations on either side of a junction interface and the mobility of oxygen or oxygen vacancies in the heterostructure.

In this join-use project, we focus on interfaces between a semiconducting oxide, $\text{Pr}_{0.8}\text{Ca}_{0.2}\text{MnO}_3$ and Aluminum metal. Under high electric fields, an electrochemical reaction can occur in solid state, resulting in the formation of an AlO_x layer at the interface, which leads to the observed reversible resistance change under electric field. As a first step in characterizing the resistance switching, it is necessary to distinguish between the effects of an interface, such as trap-related Schottky barrier height changes and the formation of point-like conduction paths, which may be related to defects or inhomogeneity in the AlO_x barrier that is formed at the interface during an initial field-driven oxidation process. In this project, therefore, the effect of the lateral junction dimensions on the junction resistance was studied. As illustrated in Fig. 1, the junction can be modeled as a series of two resistances for a pure interface device, but this does not adequately describe the observed device size dependence. Another possibility is to use a series-parallel model that also includes an effective inhomogeneity contribution in the form of a parasitic parallel resistance R' . As can be seen in the continuous-line fit curves in Fig. 1, this model gives a reasonable fit to the data.

It is known for the $\text{Pr}_{0.8}\text{Ca}_{0.2}\text{MnO}_3/\text{Al}$ system that conducting filaments do not form in the bulk of the manganites film. The junction size dependence, however, shows that a parallel conduction path does appear in the total resistance of the junctions. The most likely cause for this is the

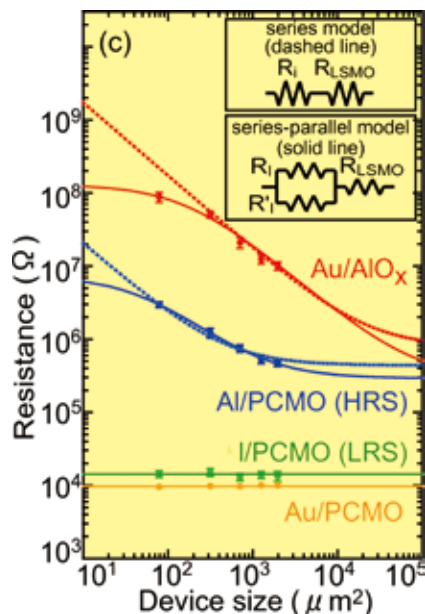


Fig. 1. Device size dependence of resistance of resistive switching junctions in the low-resistance state (LRS) and high-resistance state (HRS). In LRS, contact resistance dominates, while in HRS, only a series-parallel resistance model fit (solid lines) can reproduce the observed behavior.

inhomogeneous field-oxidation that occurs in the junctions. In order to derive intrinsic properties of semiconductor oxide/metal interfaces, nanoscale junctions may need to be used. This work also has broader implications for the design of oxide heterostructures. It is known that growing electronically clean interfaces by typical physical vapor deposition techniques is problematic due to the large number of cations that are involved at oxide-oxide interfaces. Defect formation and interdiffusion at high film growth temperatures can set fundamental limits on the sharpness of interfaces. This work shows that functional interfaces can also be built by growing heterostructures at relatively low temperature followed by the application of an electric field to prompt the movement of anions, or even cations. The electronic properties can thus be adjusted at will at room temperature after the original heterostructure has been grown.

Reference

[1] G. Sugano, I. Ohkubo, T. Harada, T. Ohnishi, M. Lippmaa, Y. Matsumoto, H. Koinuma, and M. Oshima, *Mater. Sci. Eng. B* (2009) in press.

Authors

I. Ohkubo^a, G. Sugano^a, T. Harada^a, M. Oshima^a, T. Ohnishi^b, Y. Matsumoto^c, and H. Koinuma^d

^aDepartment of Applied Chemistry, The University of Tokyo

^bNational Institute for Materials Science

^cMaterials and Structure Laboratory, Tokyo Institute of Technology,

^dGraduate School of Frontier Sciences, The University of Tokyo

Low Temperature Study of PdH_x System by Torsional Oscillator: *x* Dependent Responses

S. Harada, H. Araki, and M. Kubota

Hydrogen atoms dissolve in Pd metal [1] at densities up to one H(D) atom per Pd, which provides higher atomic H(D) density than in solid H₂(D₂). They are known to have a large diffusion coefficient due to quantum tunneling. A torsional oscillator (TO) technique is employed to investi-

gate the phases of H in Pd, which is known to show phase boundaries at the lowest *T* among metal-hydrogen (MH) systems [1]. Specific heat measurements [2,3] as well as resistivity measurements [4] have been performed for PdH_{*x*} with *x* up to ~1 specimens to establish the unique *x*-*T* phase diagram [1]. We found that vacancies at H sites cause a phase transition at low *T* in this system in the β phase [2]. We have, in addition, been performing TO experiments, a well-established, powerful method to investigate superfluidity and quantum vortices of liquid He as well as dislocation dynamics in solids. We started TO experiments in the hope to study the atomic H dynamics in the PdH(D)_{*x*} system. Our experiments have shown the resonance frequency shift and the *Q* value change for samples of PdH_{*x*}, with 0.16 ≤ *x* ≤ 0.75 at the lowest *T*. Most of the *x* linearly-dependent change in the resonance frequency can be largely explained by the lattice deformation by H intrusion [1] and by mass change by H atoms. This *x* dependent contribution is found to have [5] a much smaller additional change, but depends on *x* and *T*. We show the experimental data and discuss the origin and possible occurrence of quantum phenomena for the hydrogen system.

Study of macroscopic quantum phenomena such as superfluidity and superconductivity has a long history, and it is sometimes difficult to grasp the real advancement, yet recent progress is tremendous. Various reviews point out rapid developments occurring in superfluidity in solids [6], or superconductivity in insulators [7]. An essential component of the superfluidity (including that of conduction electrons in metals: superconductivity) in the bulk materials is Bose Condensation (BEC) of constituent particles, either ⁴He atoms or Cooper pairs of Fermions [8]. By the way, ideal gas BEC does not occur at a finite temperature for lower dimensional systems than 3D, because of stronger fluctuations. Therefore something else like Kosterlitz-Thouless mechanism has to be supposed in order to explain experimentally observed superfluidity in 2D, for example. Among the modern superfluidity phenomena, since the discovery of Cuprate High *T*_c superconductors, 2D features of the CuO₂ plane electrons play the major role for the “vortex state” of the Cuprate vortex physics [9]. Actually the vortex state, involving vortex fluid and vortex solid states is a common feature of modern superconductors, including recently

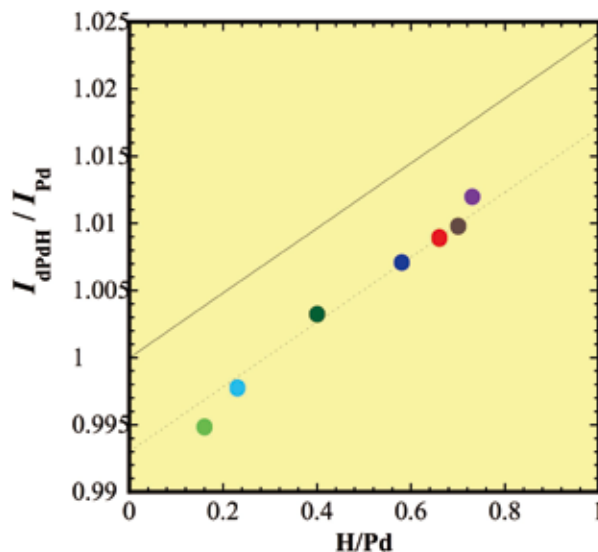


Fig. 1. The inertia ratio I_{dPdH}/I_{Pd} vs *x*, concentration of H atoms in PdH_{*x*} samples at ~5 K, the present lowest temperature. It gives a linear dependence to *x* and the slope is rather in good agreement with the estimate based on two contributions, one by expansion of the Pd lattice by H atoms, the other is the total mass change by H concentration *x*.

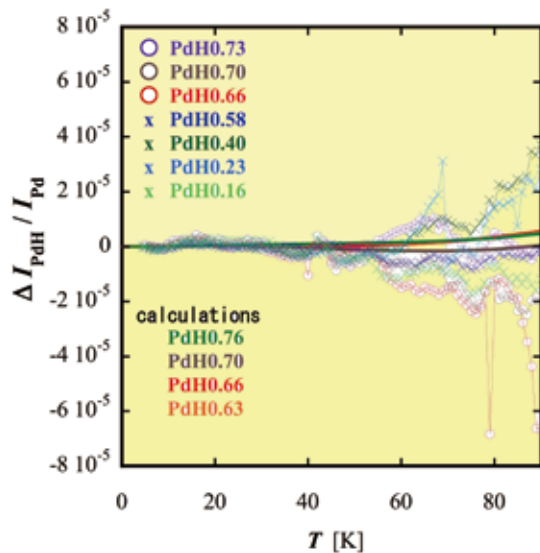


Fig. 2. Deviation from the linear x dependence of the inertia ratio $I_{\text{PdH}}/I_{\text{Pd}}$ as a function of temperature T . The size of deviation is much smaller than in Fig. 1. We have adjusted all the data to collapse on a single line near $T=5\text{K}$. To our surprise, all the data coincide up to $\sim 45\text{K}$, and then they start to fluctuate, but certainly the changes depend on x , decreasing for $x > 0.65$ (β phase \circ) and increasing for $x < 0.6$ (α phase \times). The largest change was recorded for x near 0.65 as in the specific heat peak [2].

discovered superconductivity in Fe compounds [10].

We have been interested in the PdH(D)_x system, in addition to the above given reasons, because of the reported layered structure of the O-site of the Pd fcc crystals, where vacancies of the H(D) atoms have some regular spacing [11] and this might give us some special situation to expect a new type of quantum macroscopic phenomenon.

The samples have been prepared from 4N Pd metal discs of $\sim 17\text{ mm}$ diameter and 1 mm thick, and hydrogen was electro-chemically charged at reduced temperature. Samples are mounted on a torsion pendulum made of Be-Cu using a couple of screws. Experiments were performed first for the pure sample and then the sample was charged with hydrogen to the highest $x = \sim 0.8$, then experiments are performed from the lowest $T \sim 5\text{ K}$ upwards, repeatedly. Measurements for different concentration x samples were prepared by reducing the hydrogen step-wise. Fig. 1 shows the angular momentum I_{PdH_x} divided by I_{Pd} , measured at the lowest T . The solid line in the figure has the slope calculated using the published data of lattice constant [12] and that of thermal expansion [13,14]. It is remarkable that a line through the data points for different x in Fig.1 has a slope exactly that of the solid line which is calculated by the reported data. The shift is due to the initial expansion by hydrogenation [1,13]. Actually TO has much higher resolution of the change of the moment of inertia if we take the T dependence for a single sample. Fig. 2 shows our data set for all different x 's as a function of T , where vertical position at the lowest T is adjusted to coincide to each other. There is a remarkable coincidence up to $\sim 45\text{ K}$, and then we observe different behavior depending on x with increased roughness. Samples with $x > 0.64$, in the β phase tend to show decrease of the inertia over some T above $\sim 55\text{ K}$. The two set of lines through data are the ones calculated by reported x dependent thermal expansion [13,14], which is argued to be caused by the change of the phonon modes in the PdH_x system. Our data have some common features as this evaluation involving Debye phonons for lower T and optical mode phonons originating from H at higher T (lines in Fig.2 indicate the expected inertia from the thermal expansion data [14]). Plotted data, however, show more radical nature; especially data for the β phase

samples show reduction of the inertia over a wider T range. If this is really the case we need to seek some other explanations including possible superfluidity in the atomic hydrogen system in Pd.

We plan further to investigate this system with higher resolution, stability and sensitivity.

References

- [1] Y. Fukai, "Metal-Hydrogen System" Springer Verlag (2005).
- [2] H. Araki *et al.*, J. Low Temp. Phys. **134**, 1145 (2004).
- [3] H. Araki, S. Harada, and M. Kubota, J. Phys. Chem. Solids **66** 1490 (2005).
- [4] H. Araki, Y. Sakamaki, S. Harada, and M. Kubota, Journal of Alloys and Compounds **446–447**, 436, (2007).
- [5] S. Harada, T. Donuma, H. Araki, T. Kakuta, R. Nakatsuji, and M. Kubota, presented in QFS 2010, and submitted to JLTP.
- [6] See for ex., Kubota *et al.*, JLTP. **158**: 572 (2010); and arXiv: 0903.1326.
- [7] J. G. Bednorz and K. A. Muller, Z. Phys. B **64** 189 (1986).
- [8] See for ex., A. Leggett, "Quantum Liquids", Oxford. Univ. Press (2006).
- [9] Fisher, Fisher, and Huse, Phys. Rev. B **43**, 130 (1991).
- [10] Y. Kamihara *et al.*, J. Am. Chem. Soc. **128**, 10012 (2006).
- [11] T. E. Ellis, *et al.*, Phys. Rev. Lett. **42**, 456, (1979).
- [12] J. E. Schirber and B. Morosin, Phys. Rev. B **12** 17 (1975).
- [13] H. Hemmes, B. M. Geerken, and R. Griessen, J. Phys. F, **14** 2923 (1984).
- [14] R. Abbenseth and H. Wipf, J. Phys. F, **10** 353 (1980).

Authors

T. Donuma^a, S. Harada^b, H. Araki^c, T. Kakuta, R. Nakatsuji, and M. Kubota
^a Graduate School of Sci.& Tech., Niigata University
^b Faculty of Engineering, Niigata University
^c Nagaoka National College of Technology

Pressure Induced Superconductivity in CePtSi_2

T. Nakano and Y. Uwatoko

Discovery and understanding of a new ordered state is one of the most interesting topics in condensed matter physics. As well known, in Ce-based Kondo compound, various interesting phenomena such as non-BCS superconductivity and non-Fermi liquid behavior occur around magnetic-nonmagnetic quantum critical point, when the Kondo effect overcomes RKKY interaction by changing magnetic field, chemical substitution or pressure and so on. In such sense, the antiferromagnetic (AFM) concentrated Kondo compound CePtSi_2 ($T_N = 1.8\text{ K}$, $T_K = 3\text{ K}$, $\gamma = 600\text{ mJ/molK}^2$) is a possible candidate which exhibits a new quantum phase with an application of pressure. We found a pressure-induced superconductivity in CePtSi_2 by measuring resistivity and ac susceptibility under pressure.

Figure 1 (a) displays the resistivity ρ of the CePtSi_2 sample at various pressures [1]. At ambient pressure, ρ increases with decreasing temperature, and shows two maxima at 23 K ($= T_2$) and 7 K ($= T_1$), which are well known characteristic features of Ce-based Kondo compounds affected by crystal electric field. Below 7 K , ρ decreases, and shows a sharper decrease below $T_N = 1.8\text{ K}$ due to the AFM ordering. With increasing pressure, T_N decreases and disappears above 0.9 GPa as shown in the inset of Fig. 1(b). Instead of the AFM, we found superconducting transition associated with an abrupt resistivity drop around 0.14 K above $P_c = 1.4\text{ GPa}$. This drop develops by lower current density owing to suppression of the self-heating by an excitation current as shown in the inset of Fig. 1 (a). The superconducting volume fraction is evaluated to be about 30 % from

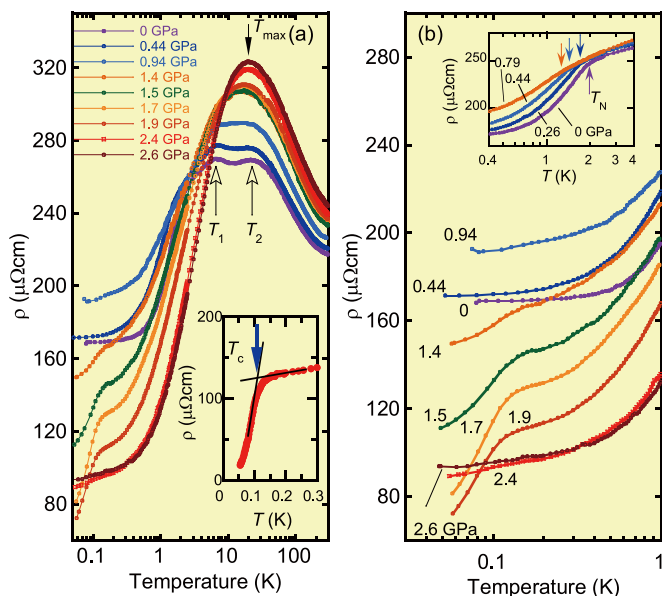


Fig. 1. The resistivity of CePtSi₂ under hydrostatic pressure. Inset: Details of resistivity around T_c at 1.7 GPa with a lower excitation current (10 μ A). (b) Resistivity of CePtSi₂ for an extended low temperature region. Inset: Details of resistivity around T_N under pressures up to 0.79 GPa. [1]

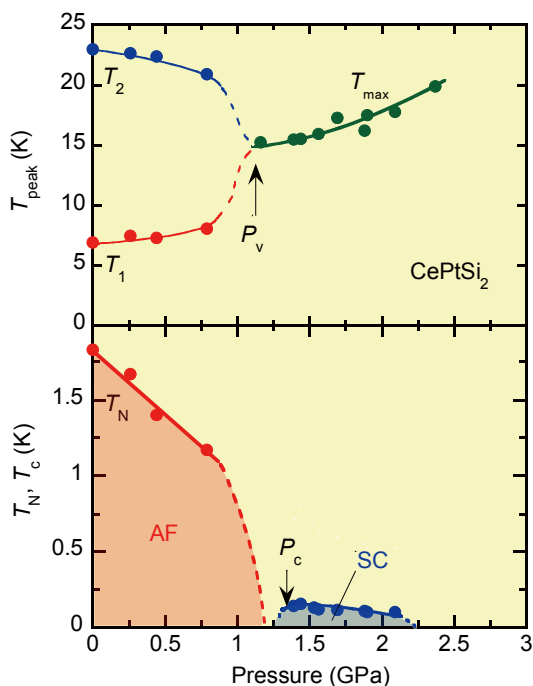


Fig. 2. Pressure dependence of characteristic temperature, T_N , T_c , T_1 , T_2 and T_{max} .

ac susceptibility, indicating that the superconductivity of CePtSi₂ should be a bulk phenomenon.

On the other hand T_1 increases with increasing pressure up to 0.9 GPa, whereas T_2 decreases. They merge into a single maximum (at T_{max}) above $P_v = 1.2$ GPa. The pressure dependence of T_1 and T_2 was reported for several Ce-based Kondo compounds.

Pressure dependences of characteristic temperatures T_N , T_c , T_1 , T_2 and T_{max} are shown in Figure 2. We can see that the superconducting phase appears just above P_v . Similar type of superconductivity is observed in CeCu₂(Ge, Si)₂ [2] etc. Jaccard *et al.* reported that the merging of T_1 and T_2 indicates an entrance in an intermediate valence state of Ce, while the T_K is of the order of the CEF splitting [2] and Miyake *et al.* have pointed the possibility of Ce-based

superconductivity due to with the valence fluctuation [3]. On the other hand, the crossover from the concentrated Kondo state to an intermediate valence state around P_v is suggested in CePtSi₂ [4,5]. These results indicate that the pressure-induced superconductivity in CePtSi₂ arises from valence fluctuation of Ce.

References

- [1] T. Nakano *et al.*, Phys. Rev. B **79**, 172507 (2009).
- [2] D. Jaccard *et al.*, Physica B **261**, 1 (1999).
- [3] K. Miyake *et al.*, J. Phys. Soc. Jpn. **57**, 722 (1988).
- [4] G. Oomi *et al.*, J. Alloys and Compd. **207**, 278 (1994).
- [5] H. Miyagawa *et al.*, High Pressure Research **26**, 503 (2006).

Authors

T. Nakano^a, G. Oomi^b, M. Ohashi^c, K. Matsubayashi, and Y. Uwatoko
^aNiigata University
^bKurume Institute of Technology
^cKanazawa University

Novel Phase Transition in CeRu₂Al₁₀

T. Nishioka, Y. Kawamura, and, Y. Uwatoko

Orthorhombic YbFe₂Al₁₀-type CeRu₂Al₁₀ exhibits a phase transition at $T_0 \sim 27$ K. This was individually found by Strydom [1] and Muro and Motoya [2] for the polycrystalline sample including some impurity phases almost at the same time. However, this compound has a low content of Ce ion that causes magnetism, so that the RKKY interaction, which leads to magnetic ordering, expected to be small. In fact, Ce compounds as low Ce content as CeRu₂Al₁₀ usually order at ~ 1 K, and thus $T_0 \sim 27$ K is extremely high as the magnetic ordering temperature.

We have succeeded to synthesize the single crystal without any impurity phase, and performed the electrical resistivity, magnetic susceptibility and specific heat measurements [3]. The temperature dependence of these physical properties indicate that partial gap as large as ~ 100 K opens over the Fermi surface below T_0 , which is similar to CDW transition. Subsequently, ²⁷Al NQR measurement reveals that this transition is due to not magnetic origin but structural one, and also confirmed the gap of ~ 100 K below T_0 [4]. These results indicate that the freedom of spin is quenched by the phase transition with non-magnetic origin.

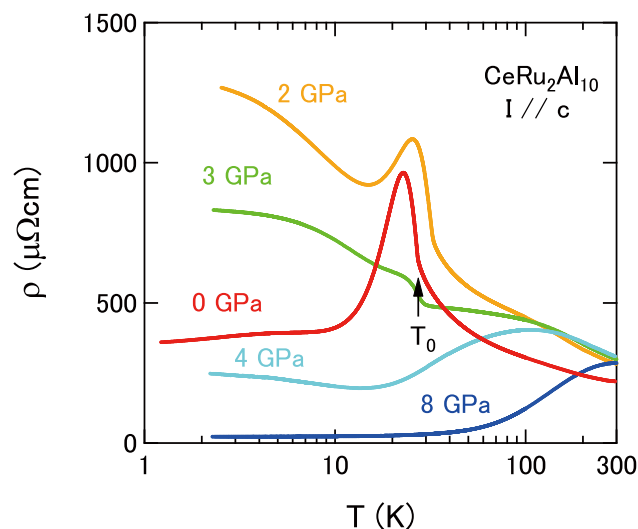


Fig. 1. Temperature dependence of ρ for CeRu₂Al₁₀ under high pressure.

Direct Spectroscopic Evidence of Spin-Dependent Hybridization between Rashba-Split Surface States and Quantum-Well States

K. He, Y. Takeichi, and I. Matsuda

In nanometer- or atomic-scale structures, size reduction implies an increase of the surface/volume ratio and the emergence of various quantum phenomena, intimately linked to the formation of electronic states different from those of the corresponding bulk materials. Recently, there have been vigorous investigations on nanometer-thick metal films, showing the quantum size effect, and on two-dimensional surfaces with large spin-orbit interactions, exhibiting the Rashba effect. In the present study, we prepared a quantum metal Ag(111) film, covered with a Rashba-type surface alloy of $\sqrt{3} \times \sqrt{3}$ -Bi/Ag, to examine mixture of these two effects, especially their spin characters.

Spin-polarized band structure of the system was investigated by high-resolution spin- and angle-resolved photoemission spectroscopy (SARPES) at KEK-PF BL-19A. The surface state (SS) bands are spin-split by the Rashba effect and hybridize with quantum-well states (QWS) in the film. The QWS subbands of the same spin orientation with the SS bands formed energy gap-openings, while those of

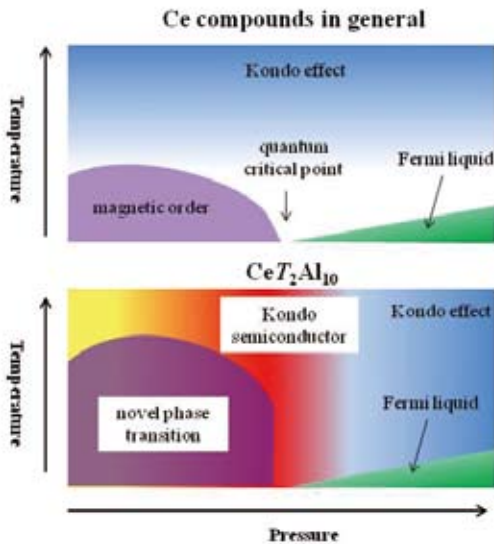


Fig. 2. Phase diagram for Ce compounds in general (upper) and that for CeT_2Al_{10} (lower).

Figure 1 shows the temperature dependence of the electrical resistivity ρ at pressures up to 8 GPa. When pressure applies to $CeRu_2Al_{10}$, T_0 passes through a maximum at ~ 2 GPa and suddenly disappears at ~ 4 GPa, where the $\rho(T)$ is similar to Kondo semiconductor. Further increasing pressure, $CeRu_2Al_{10}$ turns into a typical heavy fermion compound. The $\rho(T)$ of the related compound $CeOs_2Al_{10}$ and $CeFe_2Al_{10}$ are almost the same behavior at ~ 2 and ~ 4 GPa in $CeRu_2Al_{10}$, and the pressure dependence is what is expected from $CeRu_2Al_{10}$. Figure 2 shows a phase diagram that we propose. The origin of this novel phase transition is not probably understood by f -electron physics to date. In order to reveal this mysterious phase transition, precise thermal and transport properties [5], ultra high field magnetization [6], μ SR [7], neutron scattering [8], photoemission, ultrasonic velocity [9], low temperature X-ray measurements have been performed within one year after our discovery [1,2].

References

- [1] A. M. Strydom, *Physica B* **404**, 2981 (2009).
- [2] Y. Muro and S. Motoya, *Abstr. Meet. Physical Society of Japan (63th Autumn Meet., 2008)*, **3**, 554, 22pQC7 (in Japanese).
- [3] T. Nishioka, Y. Kawamura, T. Takesaka, R. Kobayashi, H. Kato, M. Matsumura, K. Kodama, K. Matsubayashi, and Y. Uwatoko, *J. Phys. Soc. Jpn.* **78**, 123705 (2009).
- [4] M. Matsumura, Y. Kawamura, S. Edamoto, T. Takesaka, H. Kato, T. Nishioka, Y. Tokunaga, S. Kambe, and H. Yasuoka, *J. Phys. Soc. Jpn.* **78**, 123713 (2009).
- [5] T. Tanida, D. Tanaka, M. Sera, C. Moriyoshi, Y. Kuroiwa, T. Takesaka, T. Nishioka, H. Kato, M. Matsumura, *J. Phys. Soc. Jpn.* **79**, 043708 (2010).
- [6] A. Kondo, J. Wang, K. Kindo, T. Takesaka, Y. Kawamura, T. Nishioka, D. Tanaka, H. Tanida, and M. Sera, *J. Phys. Soc. Jpn.* **79** (2010) in press.
- [7] S. Kambe, H. Chudo, Y. Tokunaga, T. Koyama, H. Sakai, T. U. Ito, K. Ninomiya, W. Higemoto, T. Takesaka, T. Nishioka, and Y. Miyake, *J. Phys. Soc. Jpn.* **79**, 053708 (2010).
- [8] J. Robert, J.-M. Mignot, G. Andre, T. Nishioka, R. Kobayashi, M. Matsumura, H. Tanida, D. Tanaka, and M. Sera, *arXiv:1003.4933* (2010)
- [9] I. Ishii, Y. Suetomi, T. K. Fujita, T. Takesaka, T. Nishioka, and T. Suzuki, *J. Phys. Soc. Jpn.* **79**, 053602 (2010).

Authors

T. Nishioka^a, Y. Kawamura^a, T. Takesaka^a, M. Matsumura^a, K. Matsubayashi, Y. Uwatoko
^aKochi University

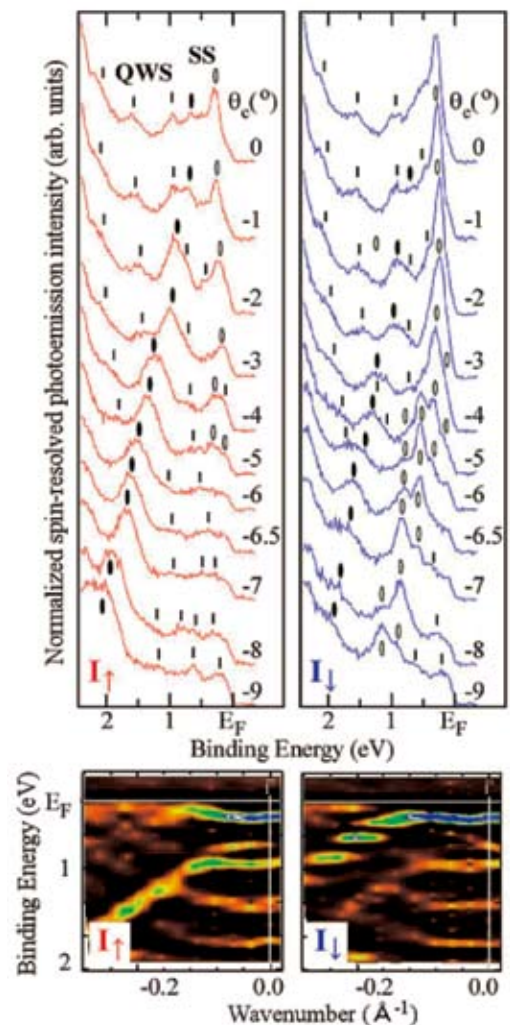


Fig. 1. SARPES spectra and band diagrams of (left) spin-up, I_{\uparrow} , and (right) spin-down, I_{\downarrow} , orientations. Dispersion of the SS and QWS bands are traced with symbols.

the opposite orientation kept the free-electron band dispersion, as shown in Fig.1. The present results give the direct evidence of the spin-dependent hybridization between the Rashba-type SS and the QWS, demonstrating that in a non-magnetic metal film the spin-degeneracy of the valence levels can be lifted by hybridization with Rashba-type SS bands.

References

- [1] K. He, T. Hirahara, T. Okuda, S. Hasegawa, A. Kakizaki, and I. Matsuda, *Phys. Rev. Lett.* **101**, 107604 (2008).
 [2] K. He, Y. Takeichi, M. Ogawa, T. Okuda, P. Moras, D. Topwal, T. Hirahara, C. Carbone, A. Kakizaki, and I. Matsuda, *Phys. Rev. Lett.* **104**, 156805 (2010).

Authors

K. He, Y. Takeichi, M. Ogawa, T. Okuda, P. Moras^a, D. Topwal^b, A. Harasawa, C. Carbone^a, A. Kakizaki, and I. Matsuda
^aIstituto di Struttura della Materia, Consiglio Nazionale delle Ricerche
^bInternational Centre for Theoretical Physics (ICTP)

Angle-Resolved Photoemission Study of Ultrathin Bi_{1-x}Sb_x Films

T. Hirahara, T. Okuda, and S. Hasegawa

Recently there has been growing interest in *topological insulators* or the *quantum spin Hall (QSH) phase*, which are insulating materials with bulk band gaps but have metallic edge states that are formed topologically and robust against any non-magnetic impurity [1]. In a three-dimensional material, the edge states become surface states and it was said that spin-split surface states of group V semimetals [2] are promising candidates for such edge states [1,3]. However as the bulk electronic structure of these materials

is not exactly an insulator, the surface-state band dispersion does not fulfill the criteria for the QSH phase edge states. There have been some theoretical proposals to open a bulk band gap for these semimetals and to realize a topological insulator [1]. One of them was to alloy antimony (Sb) into bismuth (Bi). Therefore we have prepared ultrathin Bi_{1-x}Sb_x films on a silicon (Si) substrate and measured the band dispersion using angle-resolved photoemission spectroscopy to see if a QSH phase could be realized experimentally.

The Si substrate was cut from a mirror polished *n*-type Si(111) wafer (1-10 Ωcm) followed by conventional cleaning procedures in ultrahigh vacuum (UHV) to prepare a clean Si(111)-7×7 surface. Deposition of Bi and Sb was done by resistive heating to tantalum filaments surrounding graphite tube cells. First Bi was deposited onto the Si(111)-7×7 surface at room temperature and after the formation of the (001) phase (6 bilayers (BL)) [4], Bi and Sb were co-deposited. After the deposition, the films were annealed at ~500K which resulted in a Bi_{1-x}Sb_x film showing a sharp 1×1 LEED pattern with strong spectral intensity. Photoemission measurements were performed at KEK-PF BL-18A. The homogeneity of the films (absence of segregation of Sb) and the ratio of Bi and Sb (*x*) were checked by measuring the Bi 5*d* and Sb 4*d* core level spectra at the photon energy of 50 and 80 eV. Angle-resolved photoemission measurements were performed at *hν*=22 eV using a VG-Scienta SES-100 hemispherical analyzer at ~100K.

Figures (a) and (b) show the band dispersion along the $\bar{\Gamma}-\bar{M}$ direction for the 16 BL Bi_{0.89}Sb_{0.11} ultrathin film (a), and that for the 50 BL Bi_{0.85}Sb_{0.15} ultrathin film, respectively. The electronic structure near the Fermi level is dominated by the surface states and additionally, we can observe quantum-well states in (a). The surface-state band dispersion is similar to that of the pure Bi surface state shown in Ref. [2], with a electron pocket around the $\bar{\Gamma}$ point, hole lobes along the $\bar{\Gamma}-\bar{M}$ direction, and another electron pocket around the \bar{M} point. Further analysis lead to the conclusion that the band around \bar{M} is actually composed of two different states. This fulfilled the criteria for the realization of the QSH state, which was also reported for the single crystal bulk [5].

References

- [1] L. Fu and C. L. Kane, cond-mat/0611341.
 [2] T. Hirahara *et al.*, *Phys. Rev. Lett.* **97** 146803 (2006).
 [3] S. Murakami, *Phys. Rev. Lett.* **97** 236805 (2006).
 [4] T. Nagao *et al.*, *Phys. Rev. Lett.* **93** 105501 (2004).
 [5] D. Hsieh *Nature* **452**, 970 (2008).

Authors

T. Hirahara^a, T. Okuda, A. Harasawa, I. Matsuda, and S. Hasegawa^a
^aDepartment of Physics, the University of Tokyo

Antiferromagnetic Ordering Induced by Br-Substitution in Two-Dimensional Quantum Magnet (CuCl)LaNb₂O₇

H. Kageyama, Y. Ueda, and K. Kindo

(CuCl)LaNb₂O₇ is an *S* = 1/2 square-lattice based antiferromagnet, where the magnetic CuCl layers are sandwiched by nonmagnetic LaNb₂O₇ blocks. This material has a singlet-ground state and an excitation gap of Δ = 2.3 meV [1-3]. In comparison, (CuBr)LaNb₂O₇ exhibits collinear antiferromagnetic (CAF) order at *T*_N = 32 K with

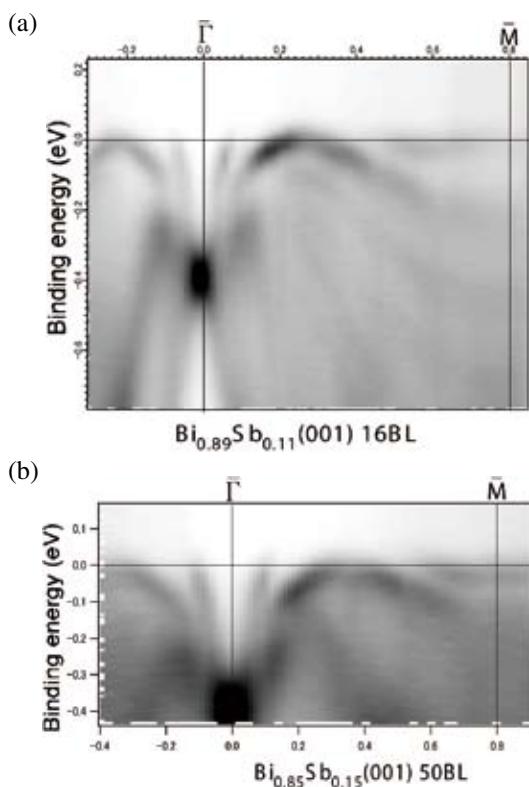


Fig. 1. Band dispersion along the $\bar{\Gamma}-\bar{M}$ direction of the 16 BL Bi_{0.89}Sb_{0.11} ultrathin film (a), and that for the 50 BL Bi_{0.85}Sb_{0.15} ultrathin film.

a propagation vector $q = (\pi \ 0 \ \pi)$ [4]. In recent studies on a solid-solution $(\text{CuCl})\text{La}(\text{Nb}_{1-y}\text{Ta}_y)_2\text{O}_7$ [5, 6], we found that the spin-singlet state in $(\text{CuCl})\text{LaNb}_2\text{O}_7$ is fairly robust against Ta substitution ($0 \leq y \leq 0.4$), accompanied by a slight reduction in the spin gap. In the intermediate region ($0.4 < y < 1.0$), we observed a quantum phase separation between the spin disordered and ordered states.

In order to obtain further insight of the spin-gap origin in $(\text{CuCl})\text{LaNb}_2\text{O}_7$, we prepared the solid-solution $(\text{CuCl}_{1-x}\text{Br}_x)\text{LaNb}_2\text{O}_7$ using an ion-exchange reaction and investigated their structural and magnetic properties [7]. In contrast to the Ta-for-Nb substitution in the nonmagnetic part, it can be expected that Br-for-Cl substitution in the magnetic part drastically changes the spin-singlet state.

Elemental analysis of the $0 \leq x \leq 1$ samples, carried out by energy dispersive spectroscopy (EDS) on a JSM-5600 scanning electron microscope, supported the nominal stoichiometry. X-ray powder diffraction patterns collected from the samples were readily indexed to the tetragonal symmetry with $a \sim 4 \text{ \AA}$ and $c \sim 12 \text{ \AA}$. The uniform distributions of the Cl and Br atoms at the X site were further supported by results of EDS on a JEM-2010F transmission electron microscopy (TEM) with an operating voltage of 200 kV. The x dependences of the lattice parameters demonstrated that both a and c change in proportion to x following Vegard's law, implying the successful preparations of the whole solid solution.

Figure 1(a) shows the temperature dependence of the magnetic susceptibility $\chi(T)$ for the solid solution. The kink at 32 K for $x = 1$ was ascribed to the onset of the CAF order [4]. Likewise, kinks were found at 17, 21, and 25 K for $x = 0.33, 0.5,$ and 0.67 , respectively. The linear decrease in the

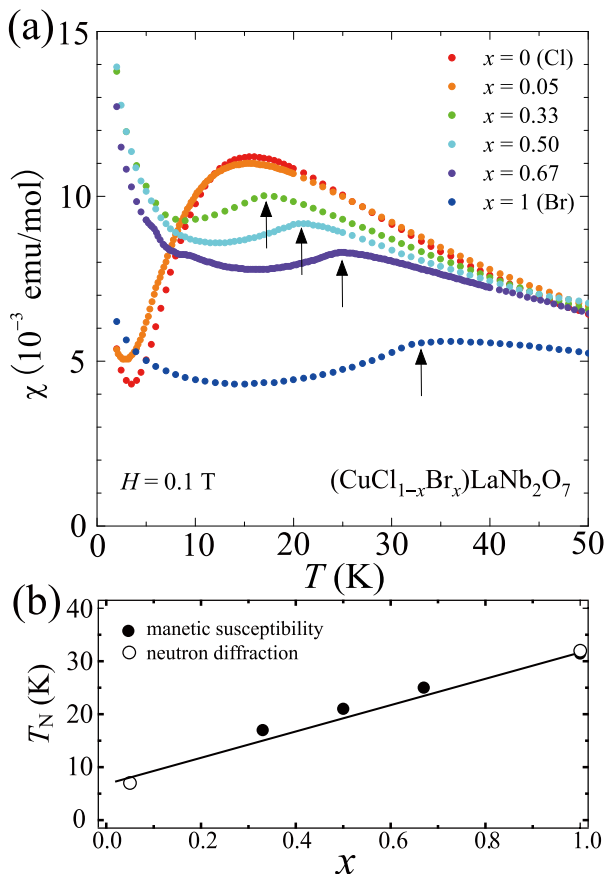


Fig. 1. (a) Magnetic susceptibility of $(\text{CuCl}_{1-x}\text{Br}_x)\text{LaNb}_2\text{O}_7$ measured at $H = 0.1 \text{ T}$. Arrows indicate the kink temperatures. (b) x dependence of $T_N(x)$, determined by magnetic susceptibility (solid circles) and neutron diffraction (open circles) measurements.

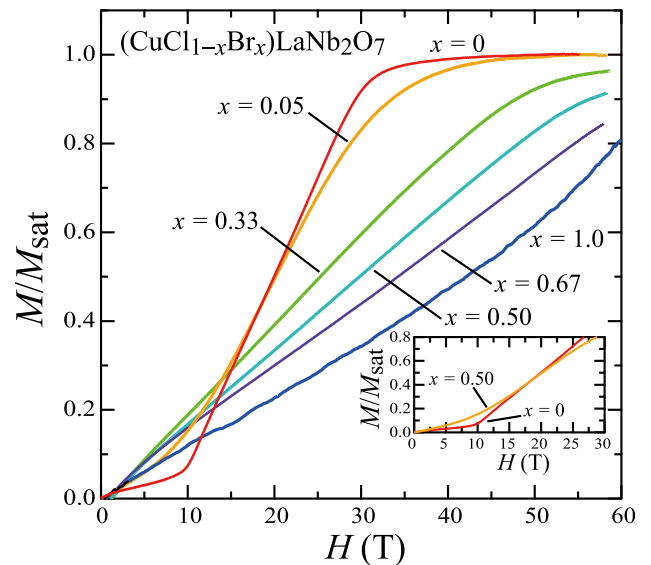


Fig. 2. Magnetization curves for $(\text{CuCl}_{1-x}\text{Br}_x)\text{LaNb}_2\text{O}_7$ measured at 1.3 K. The inset shows the magnetizations for $x = 0$ and 0.05 below $H = 30 \text{ T}$.

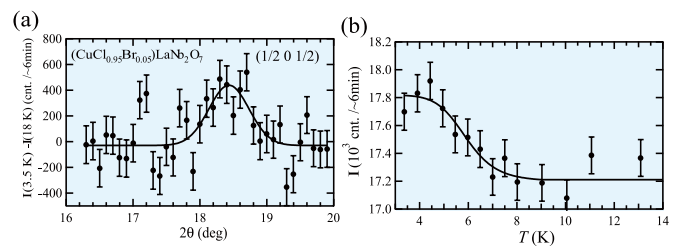


Fig. 3. (a) Difference plot of neutron scattering intensity for the $x = 0.05$ sample, $I(3.5 \text{ K}) - I(18 \text{ K})$, corresponding to the $(1/2, 0, 1/2)$ magnetic reflection. The solid curve is a single-component Gaussian fit. (b) Temperature dependence of the $(1/2, 0, 1/2)$ intensity shown in Fig. 3(a). The solid line is a guide to the eyes.

kink temperature [see Fig. 1(b)] strongly suggests that those kinks are due to magnetic order as well. In Fig. 2, the magnetization curves $M(H)$ for $x \geq 0.33$ show a linear increase over a wide field range. The saturation field tends to decrease with decreasing x , implying a weaker superexchange constant for Cu-Cl-Cu than for Cu-Br-Cu. On the other hand, both $\chi(T)$ and $M(H)$ for $x = 0.05$ are considerably different from those for $x > 0.33$. Rather, their behaviors are similar to those for $x = 0$; $\chi(T)$ for $x = 0.05$ is characterized by a broad maximum at about 15 K and substantial decrease in $M(H)$ at around 10 T is reminiscent of the transition from the spin-singlet state to the field-induced antiferromagnetic state. As shown in Fig. 3, however, the neutron powder diffraction measurements carried out for $x = 0.05$ revealed a magnetic Bragg reflection associated with $q = (\pi \ 0 \ \pi)$ same as that in $x = 1$. The temperature dependence of the $(1/2 \ 0 \ 1/2)$ intensity shown in Fig. 3(b) showed the Néel temperature is $\sim 7 \text{ K}$. Breakdown of the spin-singlet state by a small amount of Br substitution shows that $(\text{CuCl})\text{LaNb}_2\text{O}_7$ is located in the vicinity of the quantum phase boundary adjacent to the ordered state.

References

- [1] H. Kageyama, T. Kitano, N. Oba, M. Nishi, K. Hirota, L. Viciu, J. B. Wiley, J. Yasuda, Y. Ajiro, and K. Yoshimura, *J. Phys. Soc. Jpn.* **74**, 1702 (2005).
- [2] H. Kageyama, J. Yasuda, T. Kitano, K. Totsuka, Y. Narumi, M. Hagiwara, K. Kindo, Y. Baba, N. Oba, Y. Ajiro, and K. Yoshimura, *J. Phys. Soc. Jpn.* **74**, 3155 (2005).
- [3] A. Kitada, Z. Hiroi, Y. Tsujimoto, T. Kitano, H. Kageyama, Y. Ajiro, and K. Yoshimura, *J. Phys. Soc. Jpn.* **76**, 093706 (2007).
- [4] N. Oba, H. Kageyama, T. Kitano, J. Yasuda, Y. Baba, M. Nishi, K. Hirota, Y. Narumi, M. Hagiwara, K. Kindo, T. Saito, Y. Ajiro, and K. Yoshimura, *J. Phys. Soc. Jpn.* **75**, 113601 (2006).

[5] Y. J. Uemura, A. A. Aczel, J. P. Carlo, T. Goko, D. A. Goldfeld, A. Kitada, G. M. Luke, G. J. MacDougall, I. G. Mihailescu, J. A. Rodriguez, P. L. Russo, Y. Tsujimoto, C. R. Wiebe, T. J. Williams, T. Yamamoto, K. Yoshimura, and H. Kageyama, *Phys. Rev B* **80**, 174408 (2009).

[6] A. Kitada, Y. Tsujimoto, H. Kageyama, Y. Ajiro, M. Nishi, Y. Narumi, K. Kindo, M. Ichihara, Y. Ueda, Y. J. Uemura, and K. Yoshimura, *Phys. Rev. B* **80**, 174409 (2009).

[7] Y. Tsujimoto, A. Kitada, H. Kageyama, M. Nishi, Y. Narumi, K. Kindo, Y. Kiuchi, Y. Ueda, Y. J. Uemura, Y. Ajiro, and K. Yoshimura, *J. Phys. Soc. Jpn.* **79**, 014709 (2010).

Authors

H. Kageyama^a, Y. Ajiro^a, K. Yoshimura^a, M. Ichihara, Y. Ueda, M. Nishi, Y. Narumi, and K. Kindo.

^aKyoto University

Magnetization Process near the Curie Temperature of a Ferromagnetic Heusler Alloy Co₂CrGa

H. Nishihara

Self-consistent renormalized (SCR) spin fluctuation theory has successfully explained various magnetic properties at finite temperatures of weakly itinerant ferromagnets. However, the theory has difficulty such as the first order transition of the magnetization at the Curie temperature T_C . Takahashi presented an extended theory which assumes that the amplitude of the total local spin fluctuation which consists of both zero-point and thermal spin fluctuation amplitudes is conserved [1]. The theory shows that for the case of small magnetic moments, the fourth order expansion coefficient of the magnetic free energy vanishes at T_C and M^4 is proportional to H/M [1]. Such a critical magnetization process was observed in MnSi [1] and Fe_xCo_{1-x}Si, pure nickel, Ni₂MnGa [2], while the linear relation in the Arrott plot (M^2 versus H/M) was observed to be better in the case of a Heusler alloy Co₂TiGa. The issue seems to be controversial and we recently extend the study to Co₂CrGa which is one of cobalt-based Heusler alloys with a moment of 3.01/ μ_B f.u..

A SQUID magnetometer (Quantum Design MPMS-XL) with a high-temperature oven was used for measurements of the field dependence of the magnetization of Co₂CrGa polycrystals. The data showing the magnetization processes

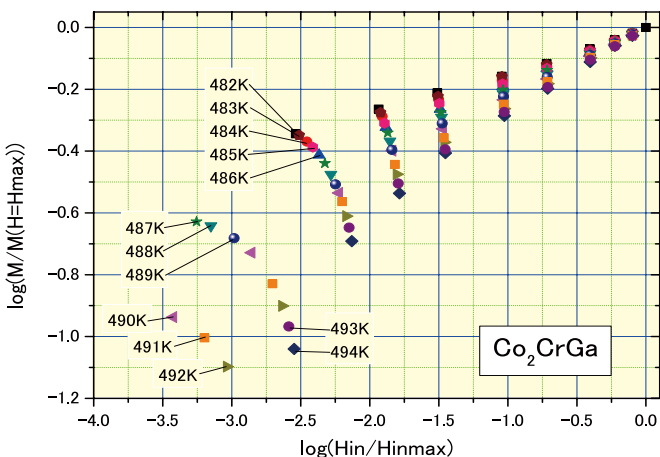


Fig. 1. The $\log(M)$ versus $\log(H)$ plots near T_C of Co₂CrGa. The externally applied fields up to 50 kOe were transformed to the effective internal fields using the demagnetizing factor. The magnetization and field are shown in normalized form.

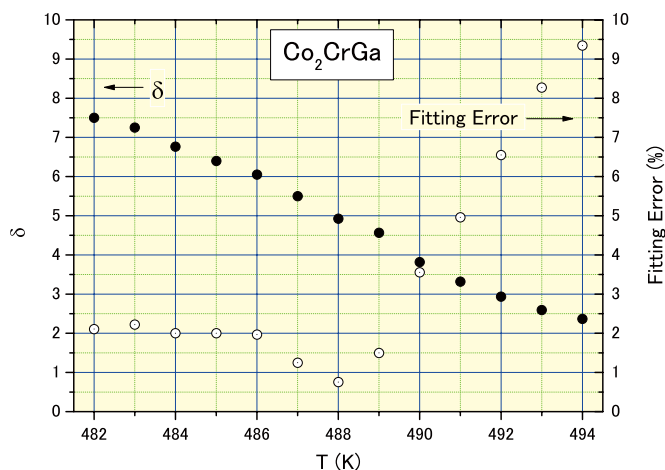


Fig.2. Each isotherm in Fig.1 is fitted to a straight line and the value of δ obtained together with the error in the fit are shown.

for various temperatures are presented in Fig.1. The critical exponent δ defined by $H = D \cdot M(T, H)^\delta$ ($T = T_C$) becomes 5.0 if theory by Takahashi is correct, while the molecular field theory predicts a δ value of 3.0. Each isotherm is fitted to a straight line and the value of δ obtained together with the error in the fit are shown in Fig. 2. From this figure, the values of T_C and δ for the Co₂CrGa sample are determined to be 488.0 (0.3) K and 4.93 (0.30), respectively. The values of δ obtained is found to be close to the theoretical value, 5.0, while the molecular field theory cannot be applied. Thus, in somewhat stronger ferromagnetic itinerant systems of pure nickel, Ni₂MnGa and Co₂CrGa, the values of δ have been found to be close to 5.0. In former times, T_C of a ferromagnet was determined by Arrott plots, but in these cases, T_C seems to be determined more accurately from the M^4 versus H/M plots which may be called “Takahashi plots”.

References

- [1] Y. Takahashi, *J. Phys. Soc. Jpn.* **55**, 3553 (1986); Y. Takahashi, *J. Phys.:Condense. Matter* **13**, 6323 (2001) and references therein.
- [2] H. Nishihara, K. Komiyama, I. Oguro, T. Kanomata and V. Chernenko, *Journal of Alloys and Compounds* **442**, 191 (2007).

Authors

H. Nishihara^a, Y. Furutani^a, T. Wada^a, T. Kanomata^b, K. Kobayashi^c, R. Y. Umetsu^c, R. Kainuma^c, K. Ishida^c, and T. Yamauchi

^aRyukoku University

^bTohoku Gakuin University

^cTohoku University

What Comes Up from Large-Scale Density-Functional Calculations

A. Oshiyama, J. Iwata, and Y. Fujimoto

Computational condensed matter science has been initiated in 80s of the previous century and contributed tremendously to the progress of physics and chemistry of materials. Density functional theory (DFT) has been a powerful tool to reveal atom-scale mechanisms for a variety of phenomena in real materials. Yet target systems which DFT has treated in the past are relatively small: calculations for 100-atom systems are typical and those for 1000-atom systems are rare at present. On the other hand, the nanometer-scale system contains more than 10,000 atoms and the nano-scale shape in the systems is now recognized as an important factor

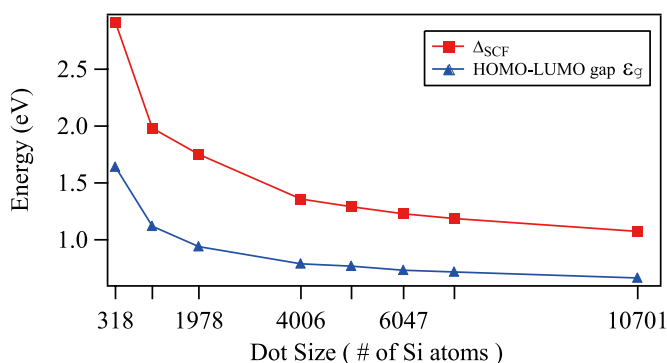


Fig. 1. Dot-size dependence of the band gap energy obtained from the Kohn-Sham level difference ϵ_g (triangles) and the total energy difference, Δ_{SCF} (squares). The diameter of the maximum dot which contains 10701 Si atoms and 1966 surface H atoms is 7.6 nm. Analysis shows the difference between ϵ_g and Δ_{SCF} is due to charging energy to the nanodots, thus both ϵ_g and Δ_{SCF} converging to the bulk band gap. Calculated discontinuity of the total energy at the integer electron number clarifies that the LDA gap is the chemical gap.

which is decisive in physical properties [1]. Hence it would be one of the most important challenges to perform DFT calculations with the levels of local density approximation (LDA) or the generalized gradient approximation (GGA) for 10,000-atom systems to clarify physics and chemistry of nano-structures.

In collaboration with computer science people at Center for Computational Sciences, University of Tsukuba, we have developed a new real-space density functional theory (RSDFT) scheme which allows us to perform total-energy electronic-structure calculations for unprecedentedly large systems containing more than 10,000 atoms on 10 TFLOPS parallel architecture computers [2]. The RSDFT scheme is essentially free from Fast Fourier Transform (FFT) which becomes a heavy communication burden in parallel architecture computers, and thus regarded as a premier scheme in the next-generation computers. We have developed several new algorithms, implemented them, and then achieved very high performance with more than 1000 CPUs.

Figure 1 shows the band gap of the Si nanodot as a function of the dot size, calculated by the local density approximation (LDA) in our RSDFT. The largest dot contains 12,667 atoms. We have calculated the Kohn-Sham level difference $\epsilon_g = \epsilon_{N+1} - \epsilon_N$ of the N -electron system and the more rigorous formula $\Delta_{SCF} = E(N+1) + E(N-1) - 2E(N)$ using the total energies E for the N -, $(N+1)$ -, and $(N-1)$ -electron systems. It is clarified that the difference of the two quantities comes from the energy cost to charge the nanodots [2].

Figure 2 is the calculated STM images for the dislocation

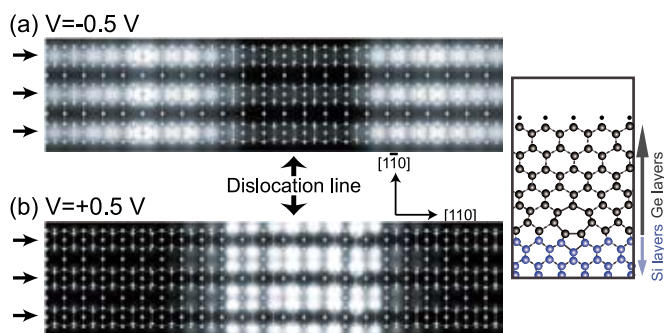


Fig. 2. Simulated STM images of the 90 degree dislocation core in Ge film on Si(001) shown in the right panel. (a) the filled-state image and (b) the empty-state image. The arrows on the left hand represent the dimer row positions. Gray and small white balls represent Ge and H atoms, respectively.

core buried at the Ge/Si interface. Strained Ge overlayers on Si substrates are important nanostructures for CMOS transistors owing to the increased mobility under strains. The pseudomorphic overlayers associated with 90 degree dislocations are good candidates to fabricate high-mobility transistors. We have identified the core structure of such dislocations by extensive structural optimization of various interface structures within LDA of RSDFT. It is found that the core structure consists of a row of pairs of 5- and 7-membered rings which releases stress energy. We have also found that the core structure is visible by STM measurements even when the Ge overlayers exist on the dislocation core.

References

- [1] A. Oshiyama and S. Okada, *Roles of Shape and Space in Electronic Properties of Carbon Nanomaterials*, in The Oxford Handbook of Nanoscience and Technology Volumes 1,2,3, (Oxford University Press, 2009).
- [2] J.-I. Iwata, D. Takahashi, A. Oshiyama, B. Boku, K. Shiraishi, S. Okada, and K. Yabana, *J. Comp. Phys.* **229**, 2339 (2010).
- [3] Y. Fujimoto and A. Oshiyama, *Phys. Rev. B* **81**, 205309 (2010).

Authors

A. Oshiyama^a, J.-I. Iwata^b, Y. Fujimoto^c
^aDepartment of Applied Physics, The University of Tokyo
^bCenter for Computational Sciences University of Tsukuba
^cDepartment of Physics, Tokyo Institute of Technology

Large-Scale Simulation of Coarse-Grained Model of Polymer Nano-Composites Rubber

K. Hagita

Prof. R. Kubo suggests importance of molecular level understanding of rubber elasticity in the famous text book “Gomu Dansei” [1]. Polymer chains of rubber are amorphous and reptate like snakes. A slow dynamics of an entangled polymer chain in a polymer melt is considered to be explained with the reptation theory by Prof. P. G. de Gennes [2], Prof. S. F. Edwards and Prof. M. Doi [3]. In experiments of polymer melts, molecular weight dependences of slowest relaxation time and viscoelasticity is proportional to $N^{3,4}$, which is stronger than that (N^3) predicted by the reptation theory, where N denotes number of segments or molecular weight in a chain. This behavior does not depend on chemical details. Therefore, we believe that excluded volume chains can reproduce this experimental result of a polymer melt and try simulation study to confirm it over many decades. Recently, the authors confirmed it by Monte Carlo simulation of bond fluctuation model [4]. Here, this model is defined on a cubic lattice. This fact indicates a certain possibility to examine complex behaviors of rubber materials by coarse-grained molecular dynamics (MD) simulations.

Here we report on our recent study on large-scale MD simulation of coarse-grained model of polymer nano-composites rubber. Recently, polymer nano-composites have attracted much interest in the viewpoints of polymer physics and science, and industrial applications. In general, a polymer nano-composite is an entangled polymer melt and/or network filled with particles and/or objects, whose size is order of 10-100 nm which is larger than the size of the entanglement length and/or the network. These fillers are used for reinforcement of the polymer nano-composite. Although this fact was discovered about a century ago, mechanism of

the reinforcement has been not understood. It is well known that these features of fillers affect morphology of fillers and behavior of confined polymers. According to recent experiments and tire rubber products, silica filler with grafting chains can realize to reduce energy loss (CO₂ emission) at 10 Hz and to increase energy loss (grip and breaking) at 1 kHz-1 MHz. Therefore, we develop new coarse-grained model of polymer nano-composite based on Kremer-Grest model [5] in order to clarify molecular level mechanism of this convenient frequency dependence. To do it, coarse grained MD simulation is expected to be a powerful tool because it can be reproduces behavior of polymer nano-composite in periodic boundary box, whose dimension is about 100 nm, during a few milli-second by using recent supercomputer.

Figure 1 shows a picture of our research plan. Positions of fillers under elongations are obtained from two-dimensional ultra-small-angle x-ray scattering experiments [6] by Prof. Y. Amemiya's group by using two dimensional pattern reverse Monte Carlo analysis [7]. These positions can be used as an initial position of fillers for coarse-grained MD simulation and reference data. We performed large-scale coarse-grained MD simulation of tire rubber as preliminary tests. We observed stress-strain relation obtained by a constant uniaxial elongation. We found that the reinforcement effect by fillers can be reproduced. In experiments, the ratio between the storage elastic modulus and loss elastic modulus is used as an index of energy loss. This

ratio can be estimated as tangent of phase-delay of stress under dynamic deformation where time change of strain is given by sine function. According to preliminary results, it is found that frequency, temperature, and amplitude dependences of this ratio seem to be qualitatively reproduced in the rubber region. Therefore, our coarse-grained model is a strong candidate of molecular-level understanding of rubber elasticity and realization of molecular-level design technique. In addition, we considered that our coarse-grained model of the polymer nano-composites can be used not only for synthetic polymer but also for repetitive amino acid chain such as spider silk.

References

- [1] R. Kubo, "GOMU DANSEI (Rubber Elasticity)", (Shokabo, Tokyo, 1947, revived 1996) (in Japanese).
- [2] P. G. de Gennes, "Scaling Concepts in Polymer Physics", (Cornell University Press, Ithaca, (1984).
- [3] S. F. Edwards and M. Doi, "The Theory of Polymer Dynamics" (Oxford University Press, Oxford, 1986).
- [4] K. Hagita and H. Takano, J. Phys. Soc. Jpn. **71**, 673 (2002); J. Phys. Soc. Jpn. **72**, 1824 (2003).
- [5] K. Kremer and G. S. Grest, J. Chem. Phys. **92**, 5057 (1990).
- [6] Y. Shinohara *et al.*, J. Appl. Cryst. **40**, s397 (2007).
- [7] K. Hagita *et al.* J. Phys.: Cond. Matter **19**, 335217 (2007); Rheo. Acta **47**, 537 (2008).
- [8] K. Hagita, Activity report of ISSP supercomputer system 2010, (2010) in press.

Authors

K. Hagita
National Defense Academy

Magnetic Monopoles in Spin Ice

H. Kadowaki, J. W. Lynn, and T. J. Sato

From the symmetry of Maxwell's equation of electromagnetism, magnetic charges or monopoles would be expected to exist and produce magnetic fields, and moving magnetic monopoles electric fields. But no magnetic monopoles have ever been observed, despite longstanding experimental searches following Dirac's hypothesis of the monopole nearly eighty years ago. Present grand unified theories predict the existence of magnetic monopoles as topological defects of the vacuum, but with enormous energies in the range $\approx 10^{16}$ GeV that preclude any hope of creating them in the laboratory. Consequently theoretical attention has turned to condensed matter systems where tractable analogs of magnetic monopoles might be found. One prediction is for an emergent elementary excitation

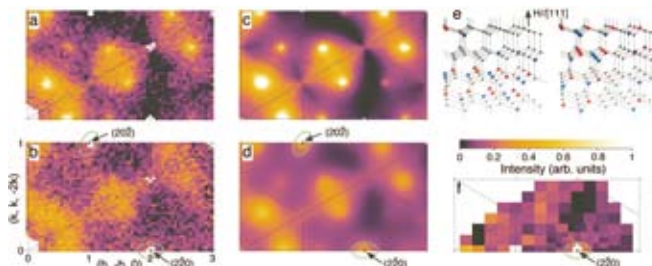


Fig. 1. Intensity maps of neutron scattering measured at $T = T_c + 0.05$ K in the scattering plane perpendicular to the [111] field (a, b, f), and corresponding MC simulation results (c, d). (a, c) Maps for the kagomé ice state at $H = 0.5$ T. (b, d, f) Maps for the fluctuating high- and low-density monopoles at $H = H_c$. (e) Two snapshots of the monopoles of the MC simulation corresponding to (b, d, f), shown on the diamond lattice connecting the centres of the tetrahedra. Blue, red and black points represents +, - and 0 magnetic charges, respectively.

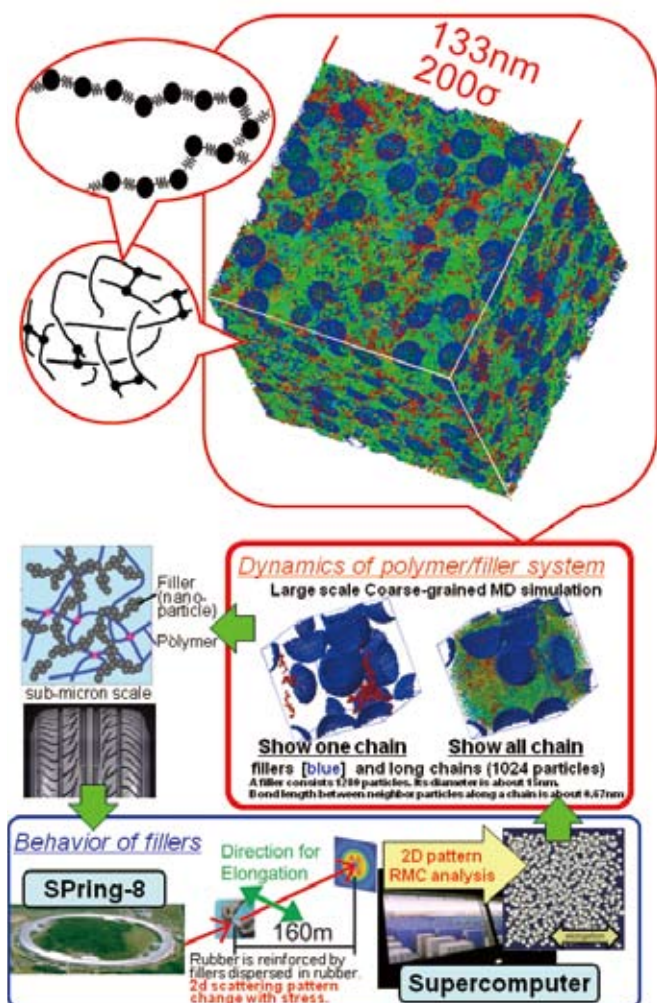


Fig. 1. Picture of our research plan for development cycle of new tire rubber and polymer nano-composites.

in the spin ice compound $\text{Dy}_2\text{Ti}_2\text{O}_7$. Spin ice is a material where the Dy spins occupy a cubic pyrochlore lattice, which is a corner sharing network of tetrahedra where the spins possess strongly competing magnetic interactions that cannot all be satisfied. This results in a ground state where two of the spins point inward and two point outward on each tetrahedron. This “2-in & 2-out” ground state spin structure has a six-fold degeneracy that follows the “ice rules”, with the possible ground states of the entire tetrahedral network being macroscopically degenerate in the same way as the famous example of disordered protons in solid H_2O , which exhibit finite entropy at absolute zero temperature. For spin ice, excitations equivalent to magnetic monopoles can be created as topological excitations from these highly degenerate ground states that represent the ‘vacuum’, with readily accessible energies of the order 10^{-4} eV.

A team of researchers from Tokyo Metropolitan University, Kyoto University, NIST Center for Neutron Research, Kyushu Institute of Technology and ISSP has used neutron scattering on a single crystal of $\text{Dy}_2\text{Ti}_2\text{O}_7$ to search for magnetic charge-type excitations in spin ice. A monopole is generated from the ground state ‘vacuum’ by flipping a spin to produce “3-in & 1-out” and “1-in & 3-out” tetrahedral neighbors, which is equivalent to a pair of positive (monopole) and negative (anti-monopole) charges sitting on the centres of the tetrahedra. The neutron experiments have confirmed the existence of the monopoles, and that they interact via the magnetic Coulomb force brought about by the dipolar interaction between spins (Fig. 1). The density of monopoles can be controlled by varying the temperature and magnetic field, and is found to follow an Arrhenius law as expected. The establishment of magnetic monopoles in this condensed matter system represents a fundamentally new type particle, and will now enable many new aspects of them to be studied experimentally in detail, such as pair creation and interaction, individual motion, correlations and cooperative phenomena.

Authors

H. Kadowaki^a, N. Doi^a, Y. Aoki^a, Y. Tabata^b, T. J. Sato, J. W. Lynn^c, K. Matsuhira^d, and Z. Hiroi

^aTokyo Metropolitan University

^bKyoto University

^cNIST Center for Neutron Research

^dKyushu Institute of Technology

High-Field Magnetization of $\text{CeRu}_2\text{Al}_{10}$

T. Nishioka, M. Sera, and K. Kindo

Recently, new ternary compounds $\text{CeT}_2\text{Al}_{10}$ ($T = \text{Fe}, \text{Ru}, \text{Os}$), with orthorhombic $\text{YbFe}_2\text{Al}_{10}$ -type structure, have attracted much attention because of the unusual physical properties. In particular, $\text{CeRu}_2\text{Al}_{10}$ is of great interest due to the novel phase transition at $T_0 = 27$ K. $\text{CeRu}_2\text{Al}_{10}$ exhibits the following characteristic features [1-3]. The specific heat, C shows a clear peak accompanied with the λ -type anomaly. The magnetic entropy obtained from the specific heat measurements is $\sim 0.65 R \ln 2$ and $R \ln 2$ at T_0 and ~ 100 K, respectively. The electrical resistivity, ρ monotonically increases with decreasing temperature and a steep increase just below T_0 , and rapidly decreases after showing a peak. The magnetic susceptibility, χ shows a large anisotropy. In the case of the magnetic field (H) parallel to the a -axis, the

Curie-like behavior can be clearly observed. Below T_0 , χ shows a decrease along all the crystal axis. The results of C , ρ and χ are well described by the thermally activated form below T_0 . This indicates the opening of a spin gap and/or a charge gap on the Fermi surface below T_0 . The magnitude of gap is estimated to be ~ 100 K.

At present, there are several candidates for the origin of a long-range order (LRO) below T_0 , such as the charge density wave (CDW) [1], the nonmagnetic structural transition [2] and the singlet pair formation between Ce ions [3]. If the LRO with a singlet ground state is realized below T_0 , it is crucial to know how is the critical field to a paramagnetic region. Therefore, it is necessary to apply the higher magnetic field up to tens of tesla in order to clarify the magnetic properties of the LRO. We performed the magnetization measurements of $\text{Ce}_x\text{La}_{1-x}\text{Ru}_2\text{Al}_{10}$ ($x = 1, 0.75$) under the high magnetic field up to ~ 55 T in order to obtain the information for the LRO in $\text{CeRu}_2\text{Al}_{10}$.

Figure 1 shows the H dependence of the magnetization (M) of $\text{CeRu}_2\text{Al}_{10}$ for $H // a$ -axis. The inset shows the magnetization curve and derivative dM/dH at 1.3 K. At 1.3 K, M shows the H -linear increase with a small slope of M up to ~ 30 T. This is probably due to the Van Vleck contribution from the excited state. With further increase of H , M shows a kink at ~ 40 T and a downward bending at ~ 50 T. Hereafter, the anomalies at ~ 40 T and ~ 50 T are called as H_c^1 and H_c^p , respectively. H_c^p is the critical field from the LRO to the paramagnetic region. These anomalies are clearly recognized by dM/dH , as shown in inset of Fig. 1. As temperature increases, H_c^p shifts to lower magnetic field. In contrast, H_c^1 becomes unclear with increasing temperature and is barely recognized above 15 K. The magnetic phase diagrams of $\text{Ce}_x\text{La}_{1-x}\text{Ru}_2\text{Al}_{10}$ ($x = 1, 0.75$) for $H // a$ -axis obtained by the present results are shown in Fig. 2. For $x = 1$, the LRO at $H = 0$ continues to exist up to 40 T. With increasing H , T_0 shifts to lower temperatures. H_c^p at 1.3 K for $x = 1$ is ~ 50 T. By La 25% substitution, H_c^p decreases down to ~ 37 T. These facts suggest that the origin of the LRO is magnetic. Quite recently, Hanzawa investigated theoretically the singlet ground state formed by the dimer of the two Ce ions with a

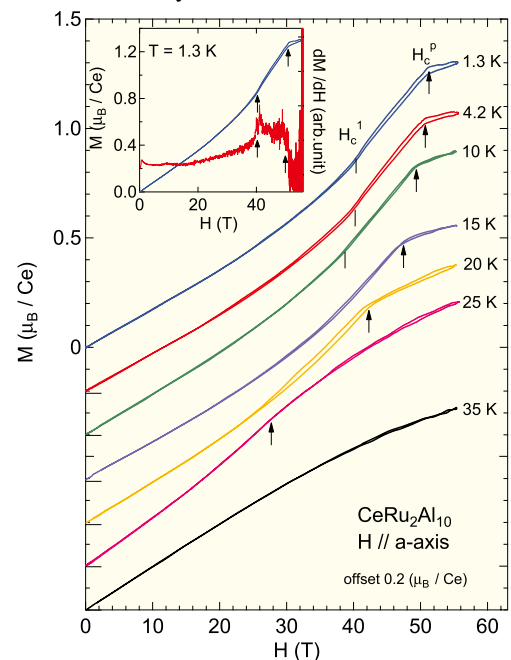


Fig. 1. Magnetic field dependence of the magnetization of $\text{CeRu}_2\text{Al}_{10}$ under various temperatures for $H // a$ -axis. The origin of the vertical axis of each curve in magnetic field is shifted so as to see it easily. The inset shows the magnetization curve and derivative dM/dH at $T = 1.3$ K.

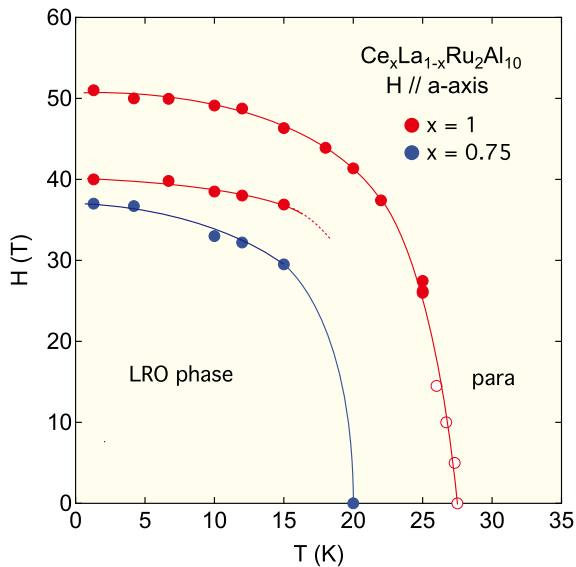


Fig. 2. Magnetic phase diagram of $Ce_xLa_{1-x}Ru_2Al_{10}$ ($x = 1, 0.75$) for $H // a$ -axis. The broken line indicates the expected phase boundary. The data (red open circle) for $x = 1$ below 15 T is cited from ref. 3.

large magnetic anisotropy in the crystal electric field (CEF) doublet ground state [4]. He assumed that two Ce ions construct a singlet ground state via RKKY interaction, and performed the mean field calculation. The H - T diagram and M - H curve obtained by the present study are qualitatively consistent with those of the mean field calculation results. These results support the recently proposed singlet ground state scenario.

References

- [1] T. Nishioka, Y. Kawamura, T. Takesaka, R. Kobayashi, H. Kato, M. Matsumura, K. Kodama, K. Matsubayashi, and Y. Uwatoko, *J. Phys. Soc. Jpn.* **78**, 123705 (2009).
- [2] M. Matsumura, Y. Kawamura, S. Edamoto, T. Takesaka, H. Kato, T. Nishioka, Y. Tokunaga, S. Kambe, and H. Yasuoka, *J. Phys. Soc. Jpn.* **78**, 123713 (2009).
- [3] H. Tanida, D. Tanaka, M. Sera, C. Moriyoshi, Y. Kuroiwa, T. Takesaka, T. Nishioka, H. Kato, and M. Matsumura, *J. Phys. Soc. Jpn.* **79**, 043708 (2010).
- [4] K. Hanzawa, *J. Phys. Soc. Jpn.* **79**, 043710 (2010).

Authors

A. Kondo, J. Wang, K. Kindo, T. Takesaka^a, Y. Kawamura^a, T. Nishioka^a, D. Tanaka^b, H. Tanida^b, and M. Sera^b
^aKochi University
^bHiroshima University

Magnetic Control of the Ferroelectricity in an Organic Spin-Peierls Material

F. Kagawa, S. Horiuchi, and M. Tokunaga

Recently, magnetically controllable ferroelectrics came into a new light due to their variety of attracting novel phenomena and also potential applications for memory devices. Most of the ferroelectric magnets have been realized in frustrated magnets in which the special kinds of magnetic order break the space inversion symmetry of the crystals. In these materials, however, the observed electric polarization (P) was considerably smaller than those in typical ferroelectric materials. Consequently, the thermodynamic properties are mostly dominated by the magnetic energy.

In this context, one-dimensional quantum magnets provide another kind of playground to study the spin-related

ferroelectricity [1]. In particular, the organic charge-transfer salt TTF-BA (tetrathiafulvalene-*p*-bromanil) has been focused as a possible candidate of the spin-Peierls (SP) ferroelectrics (see Fig. 1), whereas the presence of ferroelectricity and the magnetoelectric effects have not been studied because of the absence of sizable crystals. We studied electric and magnetic properties on newly synthesized large crystals of TTF-BA in magnetic fields (H) generated by a pulse-magnet.

The temperature (T) dependence of P and the P - E hysteresis loops clearly indicate the emergence of the ferroelectricity below $T_{SP} = 53$ K [2]. At temperatures slightly lower than the T_{SP} , isothermal magnetization (M) curves up to 56 T showed broad but finite superlinear increases in M accompanied with the changes in the slopes of the M - H curves [2], which are characteristic of the collapse of the spin-gap states in the SP systems [3]. The effect of H shows up more clearly in the P - H curves. The change in P along the b -axis of the crystal approaches $\sim 1,000 \mu\text{C}/\text{m}^2$ at 50 K in the presence of the bias voltage of 100 V as shown in Fig. 2. These results

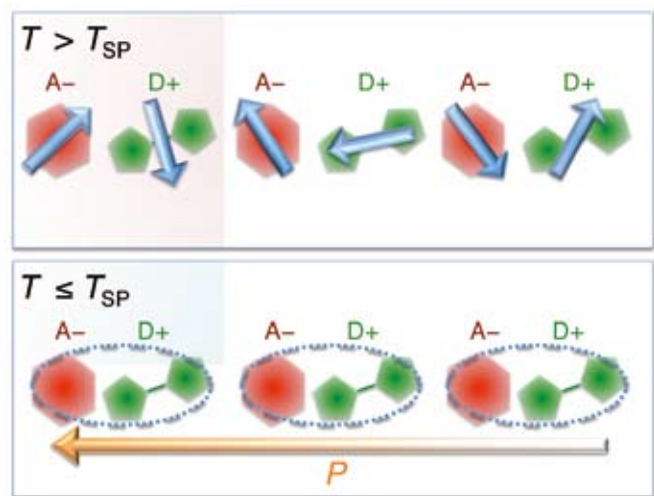


Fig. 1. Schematics of the stacks of ionic donor (D+) and acceptor (A-) in TTF-BA at above (upper) and below (lower) the T_{SP} . The blue arrow in the upper figure indicates the spin in each cite. The spins form singlet dimers below the T_{SP} . The orange arrow in the lower figure represents the electric polarization in the spin-Peierls state. Ionic displacement in the dimer phase breaks the inversion symmetry of the electric charge.

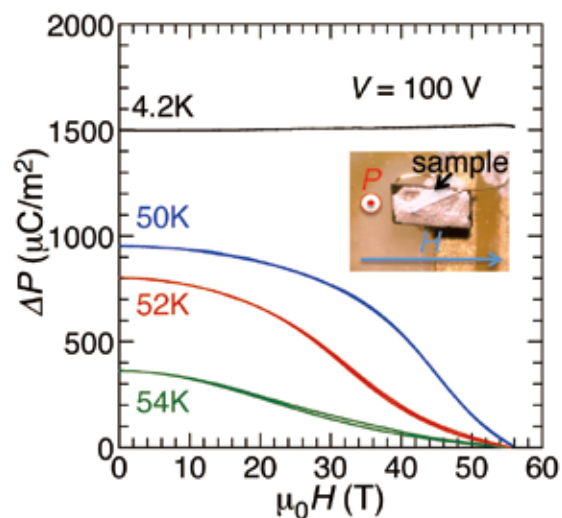


Fig. 2. Field dependence of the electric polarization (P) along the b -axis in a single crystal of TTF-BA in the presence of the bias voltage of 100 V. Magnetic fields were applied parallel to the electrode (normal to the b -axis). Application of magnetic fields of 56 T almost completely suppresses the P for $50 \text{ K} \leq T \leq T_{SP}$, whereas does not cause significant change in P at 4.2 K.

indicate that the ferroelectricity in TTF-BA originates from the instability in the quantum spin system.

On the other hand, the P shows up almost independent of H at 4.2 K. For conventional (non-ferroelectric) SP materials, the magnetic phase diagrams are known to be merged into the universal one when plotted on a reduced H - T plane. In the conventional case, the experimentally determined phase boundaries are reasonably reproduced by the Cross's theory at low fields [4]. Our results demonstrate that the ferroelectric SP phase in TTF-BA is less sensitive to the applied field than that is expected from the Cross's theory. This unusual stability of the SP state can be attributed to the strong spin-phonon coupling which may be characteristic of the ferroelectric SP system TTF-BA. It is interesting to clarify the nature of the possible soliton-lattice phase in high fields and at low temperatures [5], whereas it remains open in the present study.

References

- [1] S. Horiuchi and Y. Tokura, *Nat. Mater.* **7**, 357 (2008).
- [2] F. Kagawa *et al.*, *Nat. Phys.* **6**, 169 (2010).
- [3] As one of the examples, see M. Hase *et al.*, *Phys. Rev. B* **48**, 9616 (1993).
- [4] M. C. Cross, *Phys. Rev. B* **20**, 4606 (1979).
- [5] A. I. Buzdin, M. L. Kubic and V. V. Tugushev, *Solid State Commun.* **48**, 483 (1983).

Authors

F. Kagawa^a, S. Horiuchi^b, M. Tokunaga, J. Fujioka^a, and Y. Tokura^{a,b,c,d}

^aMultiferroics Project, Erato, JST

^bAIST, Tsukuba

^cDepartment of Applied Physics, The University of Tokyo

^dCross-Correlated Materials Research Group, RIKEN

Magneto-Optical Study of β -FeSi₂ under Pulsed High Magnetic Fields

Y. Hara and Y. H. Matsuda

Semiconducting iron disilicide β -FeSi₂ has gained a significant interest as a Si-based infrared light emitter and/or photodetector because of the 1.5 μm (0.8 eV) electroluminescence at room temperature [1]. However, the origins of the luminescence is found to be dependent on the sample; The light emission has been achieved only from β -FeSi₂ thin films synthesized by the ion beam method, whereas bulk crystals of β -FeSi₂ have not shown apparent luminescence at 0.8 eV even at low temperatures. Moreover, since the energies of the conduction band minimums at Y and Λ points are close, the nature of the energy gap (direct or indirect) is not very clear.

In order to clarify the electronic structure of β -FeSi₂ single crystals, we measured the photoluminescence (PL), optical absorption and magneto-optical absorption spectra of β -FeSi₂ single crystals. The single crystals were grown by a chemical vapor transport (CVT) method by using I₂ as a transport agent [2]. It is found that the characteristic 0.8 eV-PL bands observed in β -FeSi₂ thin films in literatures were not observed in our single crystals. However, we found new two PL lines (0.717 and 0.737 eV) and new two absorption peaks (0.858 and 0.909 eV) at low temperatures. All the samples measured in this study were classified into two groups according to the absorption peak energies. We define the sample exhibiting the PL peaks at 0.717 and 0.737 eV and absorption peak at 0.858 eV as Type A, and the sample that shows absorption peak at 0.909 eV (no PL signal) as

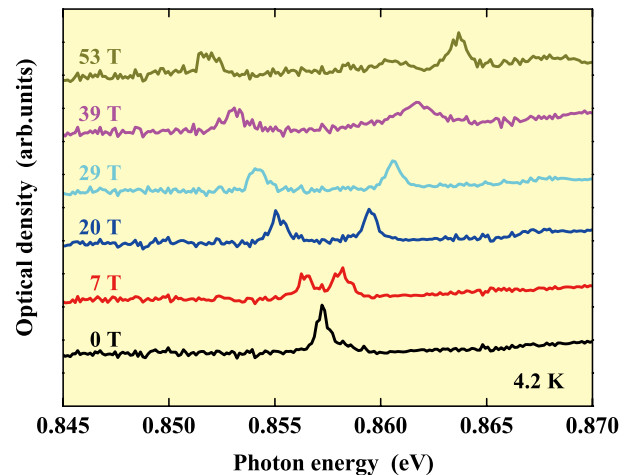


Fig. 1. Absorption spectra in Type A β -FeSi₂ in several magnetic fields. At zero magnetic field, Type A sample shows the PL peaks at 0.717 and 0.737 eV and absorption peak at 0.858 eV. The PL is too weak to measure magnetic field dependence using a pulsed magnet.

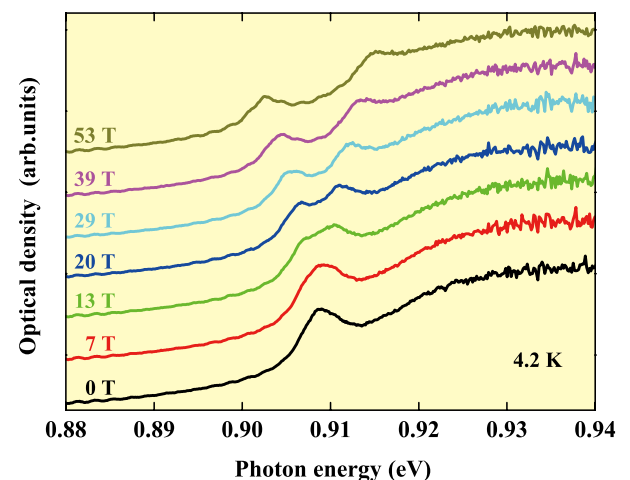


Fig. 2. Absorption spectra in Type B β -FeSi₂ in several magnetic fields. At zero magnetic field, Type B sample shows the absorption peak at 0.909 eV. The PL was not observed.

Type B. Since the origins of these new PL and absorption peaks are not clear, we made magneto-absorption experiments at low temperatures in high magnetic fields of up to 53 T. The non-destructive pulsed magnet was used for the measurement.

Figure 1 and 2 show the magnetic field dependence of the absorption spectra in Type A and Type B samples, respectively. Although the peak widths and the energy positions are very different between Type A and B, the behavior observed in magnetic fields are found to be very similar. The absorption peak splits into two peaks by applying magnetic fields. The energies of the absorption peaks of Type A and B samples are plotted as a function of magnetic field in Fig. 3. It is clearly shown that the energy between the two peaks increases in proportional to magnetic field.

The peak splitting is about 0.012 eV at 53 T for both Type A and Type B samples, resulting in the value of effective g factor to be about 4. This large g factor suggests that the absolute value of the g factor for the electrons and that for the holes are 2, which indicates that the orbital angular momentum are quenched caused by the localization of exciton wave functions at $k=0$. This result is consistent with the lacking of the diamagnetic contributions in absorption peak energy shifts indicating a very small Bohr radius of the excitons. Based on these results, the origins of the absorptions of Type A and Type B samples might be related to the

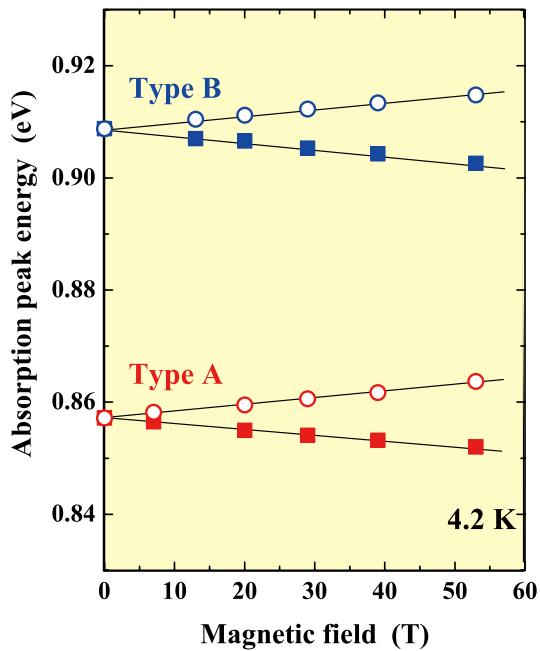


Fig. 3. Magnetic field dependences of the absorption peak energies of Type A and B samples. Both samples show the linear dependence on magnetic field, suggesting the Zeeman splitting of the localized exciton. The g factors of both samples are deduced to be about 4.

localized Frenkel-like excitons. Yamane *et al.* [3] indicated the presence of stacking faults in {100} plane (perpendicular to the incident light and the magnetic field in this study). Therefore, it is suggested that the excitons are localized at such two-dimensional (2D) stacking faults in β -FeSi₂ single crystals and the differences between Type A and Type B are caused by the local structure of the 2D stacking faults [4].

The Frenkel-like exciton as the origin of the photo absorption peaks in β -FeSi₂ single crystals is proposed for the first time. The mechanism of the PL should be closely related to the absorption process. However, the crystallographic differences between Type A and Type B samples are not examined in detail at the present. Further investigations are required to clarify the proposed localized exciton picture as the origin of the optical transitions of β -FeSi₂.

References

- [1] D. N. Leong *et al.*, Nature **387**, 686 (1997).
- [2] Y. Hara *et al.*, Thin Solid Films **515**, 8259 (2007).
- [3] H. Yamane *et al.*, J. Alloy Compd. **476**, 282 (2009).
- [4] Y. Hara *et al.*, Physics Procedia **3**, 1139 (2009).

Authors

Y. Hara^a, K. Nakaoka^a, A. Ohnishi^b, M. Sasaki^b, R. Shen, K. Kindo, S. Takeyama, and Y. H. Matsuda

^aIbaraki National College of Technology

^bYamagata University



International Conferences and Workshops

Horiba-ISSP International Symposium on “Hydrogen and Water in Condensed Matter Physics” (ISSP11)

October 12-16, 2009
J. Yoshinobu

Horiba-ISSP International Symposium on “Hydrogen and water in condensed matter physics” was held at Seimeinomori Resort (Chiba, Japan) from October 12 to 16, 2009. This was the eleventh in a series of international symposia organized by the Institute for Solid State Physics (ISSP11). ISSP11 was fully supported by UT-Horiba foundation.

This symposium offered a forum for interaction among condensed matter scientists working on hydrogen and/or water. The scientific program was designed to bring together diverse groups of researchers at the cutting edge of the field. Social events were designed to foster brainstorming across different disciplines as well as to initiate interdisciplinary collaborations. In accordance with the policy of Horiba symposium, all participants stayed for the whole period and attend every symposium during program, so that they could most effectively exchange ideas and make personal connections.

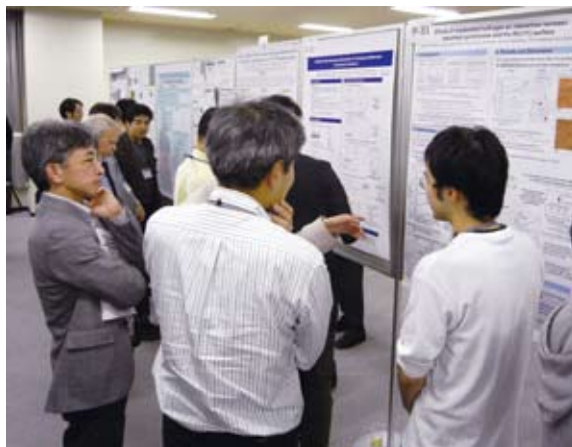
Scientific scopes and programs were arranged by the committees from various fields. This symposium covered various physical phenomena as follows.

- **Quantum behavior of hydrogen in condensed matters**
Tunneling, zero-point oscillation, ortho-para conversion
- **Hydrogen induced structural and electronic changes in solids**
Metal hydrides and hydrogen impurity in semiconductors/insulators
- **Transport of protons and electrons in condensed matters**
Fuel cells and hydrogen storage
- **Electronic structures of the water**
Liquid water and electrochemical reactions
- **Confined water**
Water molecules confined in the carbon nanotube or zeolite
- **Hydrogen and water at surfaces**
Chemical reactions on the ice and electrocatalytic reactions
- **Hydrogen and water in the soft matter**
Sol-gel transition and hydrophobic interaction
- **Hydrogen and water in the biology**
Proton pump and protein structures
- **Hydrogen and water in extreme conditions**
Solid hydrogen and hydrates

We had 22 invited lectures (Table 1), 19 oral presentations and 49 poster presentations. The total number of participants was 103. Because of high-quality poster presentations from young researchers, there were hot debates in the poster sessions. In addition, there were many opportunities for the participants to discuss intimately during the symposium.

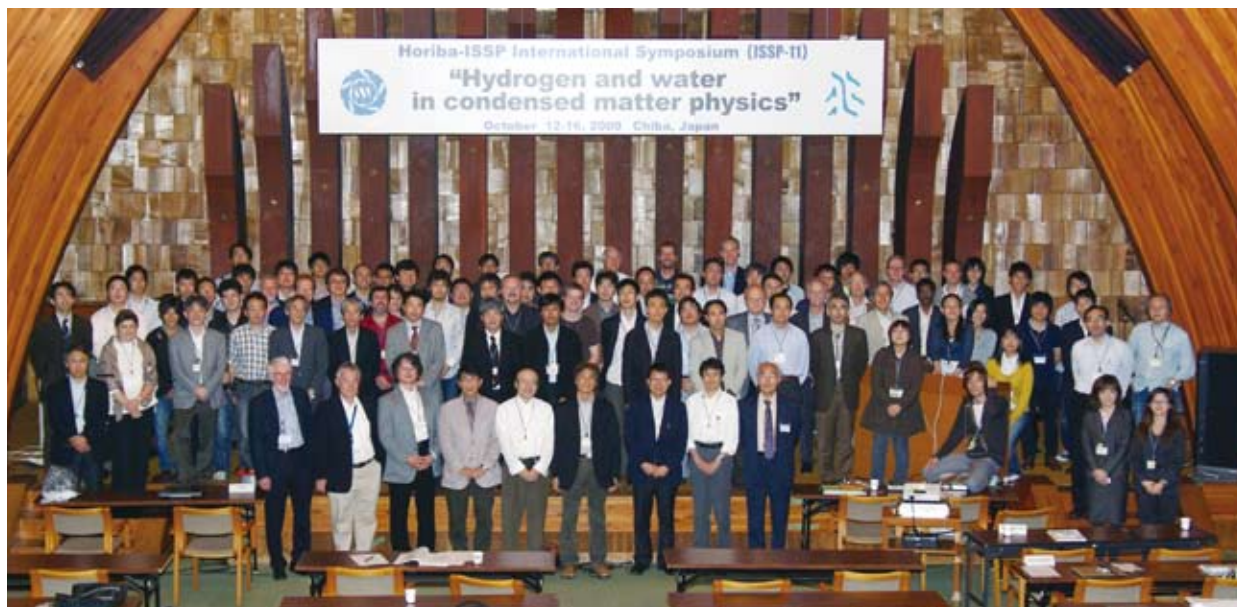
After the symposium, we received several letters of appreciation, one of which says “It was a wonderful meeting, perfectly organized, and with an outstanding scientific program - I learned a lot!”.

The details of ISSP11 are available from the web site: <http://www.issp.u-tokyo.ac.jp/public/ISSP-11/index.php>



Name	Affiliation	Title of talk
C. A. Angell	Arizona State Univ.	On the phase behavior of stretched, supercooled and glassy water, and its relation to that of other network and molecular systems
I. Chorkendorff	Tech. Univ. of Denmark	New Catalysts and Electro-Catalysts for Hydrogen Production and Conversion
A. Faraone	National Institute of Standards and Technology	Structural and Dynamical Properties of Water Confined in a Nanoporous Silica Matrix
Y. Fukai	Chuo Univ.	Iron with water/hydrogen at high pressures
Y. Furukawa	Hokkaido Univ.	Ice Crystal Growth-From Space Experiment to Biological Aspect
K. Gerwert	Ruhr-Universität, Bochum	Proteins in Action: Monitored by time-resolved FTIR spectroscopy
R. Griessen	VU Univ.	Shedding light on hydrogen
A. Gross	Univ. Ulm	Ab initio studies of hydrogen adsorption and absorption and water-metal interfaces
R. J. Hemley	Carnegie Institution of Washington	Molecules, Compounds, and Mixtures in the Hydrogen-Oxygen System at High Pressures
C. Heske	Univ. of Nevada	Soft x-ray and electron spectroscopy of the electronic structure of water and materials for photoelectrochemical water splitting
M. Kataoka	Nara Inst. of Sci. and Tech.	Effect of Hydration Water on Protein Dynamics
A. R. Khokhlov	Moscow State University	Computer Simulation of Proton-Conducting Polymer Membranes Structure and Transport Properties
K. Morgenstern	Leibniz Universität, Hannover	Ice on metal surfaces Structure and electron dynamics
M. Muthukumar	Univ. of Massachusetts	Aqueous Assembly of Polyelectrolytes
A. Nilsson	Stanford Synchrotron Radiation Lightsource	X-ray studies of hydrogen bonding in water
J. Nørskov	Tech. Univ. of Denmark	Interaction of water, hydrogen and oxygen with surfaces - understanding the water splitting and oxygen reduction processes
T. Okuchi	Okayama Univ.	Proton and hydrogen dynamics in hydrogen - bonded materials at ultrahigh pressures by high resolution diamond anvil cell NMR technique
M. Osawa	Hokkaido Univ.	Structure of Water at the Electrochemical Interface Studied by Infrared Spectroscopy
V. Pirronello	Univ. Catania	Experimental Studies of Molecular Hydrogen Formation on Surfaces of Astrophysical Interest
D. Richter	Forschungszentrum Jülich	Functional dynamics of proteins as revealed by neutron spin echo spectroscopy
M. Salmeron	Lawrence Berkeley National Laboratory	Water adsorption and reactions on metal surfaces
M. E. Tuckerman.	New York Univ.	Proton and hydroxide ion solvation and transport in aqueous environments

Table 1. Invited speakers and title of their talks



New Developments in Theory of Superconductivity

June 22-July 7, 2009
K. Ueda and H. Tsunetsugu

The fourth International Workshop organized by the ISSP theory group focused on “New Developments in Theory of Superconductivity”. The workshop was held at ISSP for three weeks from June 22 through July 7 in 2009. The last three days of the workshop was devoted to the symposium on the subject.

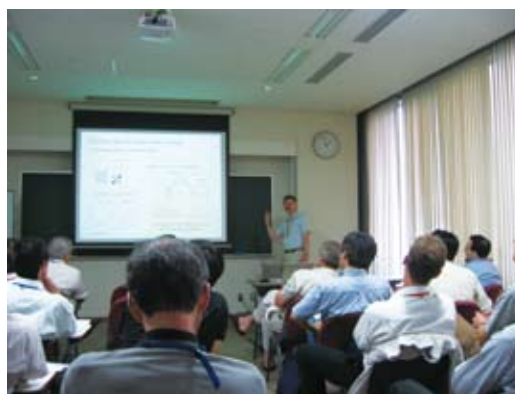
Discoveries of new type of superconductors have been a strong motive force for developing new ideas of novel type of superconductors, especially new mechanism of superconductivity. Recent discoveries of iron pnictide superconductors and superconductivity in non-centrosymmetric metals are a few of recent examples and these subjects were discussed in the workshop intensively. In addition to these subjects the effects of proximity to quantum criticality and the effects of anharmonic phonons were also central topics of the workshop.

Several excellent lectures were also given by experimentalists. These lectures which reviewed recent important experimental developments were very useful and stimulated active discussions among the participants.

The workshop was sponsored by ISSP, Global Center of Excellence for Physical Sciences Frontier, University of Tokyo, and Scientific Research on Innovative Areas “Emergence of Heavy Electron and Their Ordering”, MEXT.

The program and other details of the Workshop can be found at the Workshop web page URL.

<http://www.issp.u-tokyo.ac.jp/public/ndts/index.html>



IPMU Focus Week “Condensed Matter Physics Meets High Energy Physics”

February 8-12, 2010

H. Aoki, H. Ooguri, M. Oshikawa, T. Takayanagi, and S. Ryu

Interesting developments in science, especially in theoretical physics, often take place at boundaries of different disciplines. The interaction between condensed-matter physics and high-energy physics has been particularly fruitful, as it is evident in Yoichiro Nambu’s work which was awarded Nobel Prize in Physics in 2008. Recently, there arose renewed strong interests in this interface. Examples include AdS/CFT correspondence, which surprisingly relates quantum critical points to classical gravity.

Institute for Physics and Mathematics of the Universe (IPMU) in the University of Tokyo is recently launched for studies in high energy physics, cosmology, and related mathematics, created under the JSPS WPI program. The new permanent building of IPMU was just completed in December 2009 right next to ISSP. As an inaugurating international workshop at the IPMU, the workshop “Condensed Matter Physics Meets High Energy Physics” was organized in cooperation with ISSP. This is indeed a very fitting venue to host the interdisciplinary workshop between the two fields.

The number of participants reached approximately 200, reflecting the vigorous interests in the both communities. Among them, approximately 40 participants came from 12 different countries abroad. In addition to invited and contributed talks, several pedagogical lectures were given, in order to enhance communications between the two fields. Moreover, a panel discussion was organized to list important open questions hovering around the interface, to be studied in the near future.

The main topics discussed at the workshop include topological superconductor/insulator, AdS/CFT correspondence and its applications to condensed matter systems, and quantum entanglement in many-body systems. It was remarkable, and symbolizes the interdisciplinary nature of the workshop, that experimental data on condensed-matter systems often appeared in the presentations – mostly in those given by high-energy physicists! Lively discussions took place during coffee breaks and after hours. So the workshop has stimulated the interdisciplinary activities, and we hope that this is just a kickoff in the collaboration between IPMU and ISSP.



ISSP Workshops

Dynamics Induced by New Excitation Sources at Surface and Interface

June 19, 2009

Y. Matsumoto, T. Munakata, H. Okuyama, F. Komori, and J. Yoshinobu

Various excited states play important roles in the dynamical processes at the surface and interface, such as charge transports and chemical reactions. For their microscopic understanding, it is indispensable to clarify the non-adiabatic processes in the transitions among excited and ground states. Recently, new spectroscopic methods have been developed by using high-brilliance synchrotron light and ultra-short pulsed laser, and are now applied to the studies on the dynamics at the surface and interface. Moreover, striking developments in the first-principles calculations, for example, the formulations of the dynamical processes at the liquid-solid interface and its application of the excited states, make it possible to discuss the experimental results microscopically. Thus, we are now at the stage for pursuing intensive studies on the dynamics at the surface and interface both experimentally and theoretically to understand the adiabatic processes in a unified way. This will also largely contribute the application areas including photo catalysts, solar cells, organic devices, and so on. In the workshop, 15 speakers presented their recent results, and more than 40 attendants discussed the future prospects of this research field.

New Developments in Theory of Superconductivity

July 8-10, 2009

K. Ueda and H. Tsunetsugu

This ISSP workshop was held as a part of the international workshop of the same title. See the section of “International Conferences and Workshops.”

Development of Material Science by Frontier Spectroscopy with Brilliant VSX Source

July 23-24, 2009

I. Matsuda

Recently there have been remarkable progresses in experimental researches with high-brilliant vacuum ultraviolet ~ soft X-ray (VSX) synchrotron radiation sources. Among the various frontier VSX spectroscopy techniques, the present workshop focused on 1) soft X-ray emission spectroscopy, 2) time-resolved soft X-ray spectroscopy, and 3) nanometer-region spectroscopy. Twenty six scientists were invited to present their recent investigations and they discussed the experimental advances with the audience. The workshop was composed of the following sessions.

- 1) Status and future of nano-spectroscopy methods
- 2) High resolution soft X-ray emission spectroscopy and the future developments
- 3) Real time observations by time-resolved soft X-ray spectroscopy and imaging techniques
- 4) Researches on electronic properties of organic devices
- 5) The University-of-Tokyo Synchrotron Radiation Outstation Beamline

In the session 5), schedule and design of a new high-brilliant soft x-ray beamline, SPring-8 BL07LSU, that would be constructed at SPring-8 in October, 2009, were described. Posters of the beamline and the experimental end-stations were also exhibited at the site. The participants, especially young scientists, showed their high expectations for the state-of-the-art spectroscopy techniques with new high-brilliant photon sources and they engaged in a lively exchange of opinions regarding the future experiments through the workshop.

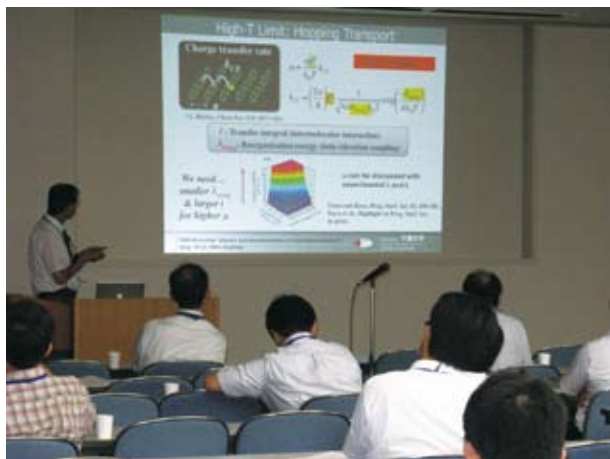


Physics and New Phenomena of π -electronic Interfaces

August 10-12, 2009

N. Ueno, H. Tajima, T. Hasegawa, and J. Takeya

Physics of interfaces for organic materials has progressed enormously in recent decades as a result of worldwide activity on organic devices. This field is a young and rapidly growing field, and researchers working in this field have various background — surface science, device physics, solid state physics of organic materials, etc. This workshop was organized to bring them together to discuss various aspects of the interface problems as well as new developments in experimental techniques. Topics discussed in the workshop included: clean and well-organized π -electronic interfaces; photoelectron and related spectroscopy; interfacial charge transport; surface/interface structures; electronic states and phase transitions; molecular semiconductors; carbon nanotube and graphene; organic transistors and other devices. We had 160 participants in total, 28 oral (including 5 invited speakers from abroad) and 18 poster presentation. This workshop was organized under the auspices of GCOE (Chiba University), AIST, Osaka University, and ISSP.



Dirac Electron Systems

October 22-24, 2009

H. Fukuyama, T. Ando, T. Enoki, R.Saito, S. Tarucha, H. Fukuyama, T. Osada, Y. Hasegawa, and F. Komori

Since the realization of single-layer graphene by cleaving graphite, novel electronic properties of graphene have been intensively studied as a typical example of massless Dirac electron systems in solids. Now, in addition to the cleaved and epitaxial graphenes, a molecular conductor α -(BEDT-TTF)₂I₃ and topological insulators are studied in detail as other Dirac electron systems with different parameters. We expect further progresses in the studies on their electronic properties such as spin-polarized edge states, fractional quantum Hall effect, residual conductivity at Dirac point, and anti-localization in these materials. The subject of this workshop was electronic properties of these Dirac electron systems. Recent experimental and theoretical results were presented by 59 speakers, and various aspects of Dirac electron systems were discussed. This workshop stimulated further progress of the research and mutual understanding among the researchers in this newly-developing and interdisciplinary field.

Supercomputer Joint Use Activity Report 2009

December 10-11, 2009

O. Sugino, N. Kawashima, H. Noguchi, S. Tsuneyuki, Y. Yoshimoto, T. Duzuki, Y. Tomita, Y. Noguchi, and H. Shiba

This is an annual workshop for joint use of ISSP supercomputer facility. The 2009 workshop consisted of the annual session, where the users reported their recent progress in developing computer code and/or in scientific output, and the symposium, where active researchers dealing with very large-scale supercomputing provided recent activity and gave comments on how the next generation supercomputer will change the condensed matter study. The invited speakers therein consisted of younger researchers, mostly research associate or post-doc, and emphasis was put on practical aspect of the computational research when compared with the past workshops. The symposium contained also special session for GPGPU (General-purpose computing on graphics processing units) which has been attracted as a kind of vector type computer. The talks consisted of scientific application, computer center management, and manufacture. They were carefully prepared for the audience to understand how GPGPU boosts some of the numerical study and how future GPGPU needs modification for more general purpose usage. More than 120 attended the workshop.



ISSP workshop “New Opportunities in VUV Solid State Spectroscopy by Improving PF BL19 Undulator Beamline”

December 18, 2009

J. Yoshinobu, A. Kakizaki, and I. Matsuda

The undulator beam line BL19 at Photon Factory has been maintained by the Synchrotron Radiation Laboratory of ISSP and opened to joint-research experiments since 1986, and the renovation of the undulator is now under the consideration to meet further needs of the better performance. This ISSP workshop was organized to discuss the renewal of BL19 and the new opportunities in condensed matter physics using synchrotron radiation in VUV (10-250eV) region. New designs for the beamline were proposed including an electromagnetic undulator and a high-resolution monochromator. The current statuses of VUV beamlines in other synchrotron radiation facilities, such as those in UVSOR (Institute for Molecular Science) and HiSOR (Hiroshima University) were also reported. In the workshop, several state-of-the-art experiments using VUV spectroscopy and new scientific opportunities to be promoted in the beamline were vigorously discussed by the participants with high expectations of BL-19 renovation project.

IPMU Focus Week “Condensed Matter Physics Meets High Energy Physics”

February 8-12, 2010

H. Aoki, H. Ooguri, M. Oshikawa, T. Takayanagi, and S. Ryu

See the section of “International Conferences and Workshops.”

ISSP workshop on “Progress on Nanoscale Spectroscopy and Nanoscience”

February 22-23, 2010

T. Kinoshita, Y. Watanabe, E. Okamura, T. Koshikawa, N. Yamamoto, T. Sekiguchi, and Y. Hasegawa

Recent rapid progress in nanoscale-controlled devices and materials demands characterization of various physical/chemical properties, not just only on morphology, atomic arrangement or chemical composition but also on electronic, electrical and magnetic/spin structures in high spatial resolutions. The workshop focusing on various nanoscale spectroscopic tools, such as low-energy scanning electron microscopy (SEM), scanning tunneling spectroscopy (STS), infrared near-field microscopy, spin-polarized low energy electron microscopy (SPLEEM), photoemission spectroscopy using a X-ray nano-beam, and photoelectron emission microscopy (PEEM) using synchrotron-radiation light source, was held with an intention of mutual communication and share on physics/chemistry and technical know-how on the methods for future collaborations among related researchers who have diversified research backgrounds and thus otherwise small chances to get together. Cutting-edge advancements on various nanoscale characterization methods were presented by young active scientists who have developed and operated the tools. Researchers who fabricate nanoscale materials/devices such as semiconducting nano wires and spintronics devices discussed their high expectations toward further developments and new functions on the nanoscale characterization. Theoretical scientists proposed new unique nanoscale phenomena, which might be observed with the tools. With 19 talks and 26 posters and more than 80 participants including 20 from industry, the discussion at the workshop was very active and fruitful, indicating strong interests in the fields.



Quantum Solid properties, the Supersolid state, and the Vortex State

March 5-6, 2010

A. V. Kuklov, S. Nemirovskii, E. Kim, M. Tsubota, M. Uwaha, and M. Kubota

The supersolid (SS) state is characterized both by the real space symmetry of a lattice structure and by the momentum space ordering of superfluidity. Originally arguments were based on the Bose-Einstein Condensation (BEC) of the imperfections as vacancies, interstitials, and other excitations in the quantum solid, where the average particle displacement caused by the large zero point motions, (25 % of the lattice constant for ex. solid He), surpasses the classical melting condition. Following the theoretical consensus about the supersolid occurrence in solid He around 1970, there had been world-wide experimental searches, but in vain. The situation dramatically changed with the report by Kim and Chan (2004) on the possible observation of "non-classical rotational inertia (NCRI)", but a microscopic explanation is still lacking. It is becoming increasingly clear that we do observe the vortex fluid (VF) state as seen in the "new type of superconductors", as Cuprate High T_c Superconductors (HTSC). This ISSP workshop developed from discussions with Prof. Kuklov, who tries to construct a microscopic supersolid theory of the dynamics of imperfections such as dislocations and others, and with Prof. Sergey Nemirovskii, with whom the ISSP Kubota group could analyze the torsional oscillator experiment results in terms of quantized vortex dynamics. We had Professors E. Kim (KAIST, Korea), and K. Shirahama(Keio) among the participants(a total of 59=33+26 registered), who contributed as specialists in quantized vortices and quantum solids and are listed in the following url as in the abstract booklet.

See also http://www.issp.u-tokyo.ac.jp/cgi-bin/n1004_edetail.cgi?c=short_term_society_table::158

And “Program+Abstracts” in above url.

